UNIVERSITY OF OKLAHOMA

GRADUATE COLLEGE

NETWORK SCIENCE APPLICATIONS IN INDUSTRIAL ORGANIZATION

A DISSERTATION

SUBMITTED TO THE GRADUATE FACULTY

in partial fulfillment of the requirements for the

Degree of

DOCTOR OF PHILOSOPHY

By

KASRA KHADEMOREZAIAN
Norman, Oklahoma
2024

NETWORK SCIENCE APPLICATIONS IN INDUSTRIAL ORGANIZATION

A DISSERTATION APPROVED FOR THE
DEPARTMENT OF ECONOMICS

BY THE COMMITTEE CONSISTING OF

Dr. Georgia Kosmopoulou, Chair

Dr. Myongjin Kim

Dr. Qihong Liu

Dr. Sridhar Radhakrishnan

Dedicated to my mother, Atty.

Acknowledgements

I am deeply grateful to Dr. Georiga Kosmopoulou, for her unwavering support, guidance, and patience throughout my studies. This dissertation would not be possible without her. I would like to express my gratitude to my coauthors: Dr. Georgia Kosmopoulou, Dr. Carlos Lamarche, Dr. Qihong Liu, Dr. Myongjin Kim, and Dr. Lei He. I would like to extend my heartfelt thanks to my committee members: Dr. Georgia Kosmopoulou, Dr. Qihong Liu, Dr. Myongjin Kim, and Dr. Sridhar Radhakrishnan. As my professors, your mentorship and insightful comments have been invaluable to my growth and the completion of this dissertation. I am very grateful to my family and friends for their support and motivation. Your encouragement and care have been my strength throughout this journey.

Contents

List of Tables

List of Figures

Abstracts

In recent years, CryptoArt prices have surged to levels typically associated with renowned artists' works, a phenomenon both puzzling and understudied. The first chapter investigates how trading networks and platform connections influence prices in the digital art marketplace hosted on the Foundation platform. We find that larger seller trading networks lead to higher auction prices for lower priced digital art, while platform connections play a critical role, especially for the most expensive pieces. Our research underscores that in decentralized online markets, the power to set prices rests with trading networks and platform connections, with differential impact across the distribution of prices.

In the second chapter, we examine the dynamics of repeated NFT auctions on the Foundation platform, focusing on how buyer and seller reputation and experience—measured by the number of followers and Katz centrality—impact resale prices. Our findings reveal that the popularity of sellers in primary sales who is also the creator of digital art positively influences both resale prices and the likelihood of resale. The trading experience of buyers raises relative prices but negatively affects the likelihood of trade in matched samples. Extensive trading networks among buyers show varied effects on resale dynamics, demonstrating cautious consideration of opportunities to buy but aggressive bidding behavior when they do. This study provides valuable insights into the evolving digital art market, highlighting factors that drive resale likelihood and prices, and contributing to a deeper understanding of digital asset

markets and their parallels with the traditional art market.

In the third chapter, We investigate the route network decisions made by airline carriers in the United States, considering both direct and indirect flights and the interdependencies of the markets. Our modeling approach allows us to analyze airlines' decisions regarding their entire route networks, rather than focusing solely on individual market choices. We estimate the likelihood of selecting a route network based on the past network, competitors' networks, and route characteristics. We find that routes facilitating greater opportunities for indirect flights are more likely to be served by airlines, and competition increases the likelihood of serving a route.

Chapter 1

Networks, Platforms, and Auction Pricing: Evidence from the NFT Art Market

Non-Fungible Tokens (NFTs) have surged in popularity in recent years, commanding prices that sometimes reach millions of dollars (Kireyev and Evans, 2021). In the domain of NFTs, one prominent category is CryptoArt, enabling artists to bypass traditional intermediaries typically found in conventional art auctions. Transactions take place on an online platform where users can access information, engage in auctions, or offer their artwork for sale. These platforms also serve as information hubs, facilitating users in accessing details about artworks, artists, and supplementary sources of information such as social media accounts. This capability enables bidders to collect information about past transactions and the popularity of rivals and sellers, information not typically available in traditional auctions.

Platform rules foster the development of a decentralized network whose impact on information diffusion can be fundamentally distinct from that of traditional art markets where dealers, as market makers, play a central role in shaping market outcomes. De Silva et al. (2022a) studied trading networks in a traditional art market using a historical dataset of auctions taking place in London in a span of a century and a half. By examining the development of networks of art dealers and their subsequent influence on artwork prices, they considered factors such as network size and depth of interactions among participants. Their findings suggest that a larger and more interconnected dealer network intensifies informational imbalances among buyers to the benefit of informed dealers.

In the context of the decentralized market for digital art NFTs, platform connections characterized by follower and following interactions, take on a new dimension of importance beyond trading networks. The survey paper by Grover et al. (2022) on the evolution of social media influence underscores the limited exploration in the literature of topics such as information diffusion, and competitive influence in a market context. Etter et al. (2019) and Rapp et al. (2013) established that social media facilitates individuals in building public perception to increase their reputation in the market. Within these digital connections, users amass social capital, which can be effectively leveraged for the purposes of disseminating information and exerting influence over others. The distinctive features of NFT platforms, their reliance on digital connections, and the interdependence among auction participants offer an opportunity to examine how information diffusion and competitive influence affect market outcomes.

Our investigation reveals that in the market for digital art NFTs, information diffusion through various network connections plays a pivotal role in shaping prices. The theoretical model representing this auction environment was initially developed by Milgrom and Weber (1982) and further generalized by Hong and Shum (2003) to an asymmetric framework. Theory suggests that information leads to aggressive bidding, resulting in higher auction prices. What the theory does not predict definitively is how bidder asymmetries (e.g., in trading experience or popularity) will manifest across the distribution of prices, with the exception of Maskin and Riley (2000) and De Silva et al. (2003) who offer insights when distributions exhibit stochastic dominance. Our basic empirical modeling structure allows us to explore the differential impact of trading networks and platform connections across the winning bid distribution.

The NFT market has witnessed significant fluctuations in the valuation of digital art, experiencing both rapid growth and subsequent decline. The market we analyze is characterized by a widespread price distribution, with values ranging from an average of \$51 (10 least expensive NFTs) to \$1.15 million (10 most expensive NFTs). While it is possible to use standard regression to investigate the effects of networks on prices (as in, e.g., Vasan et al. 2022), the approach is not informative to study how networks impact the most expensive NFTs. We employ instead semiparametric methods that allow us to obtain point estimates at different price points or quantiles of the distribution (Chernozhukov et al., 2024; Lamarche and Parker, 2023). Furthermore, our approach enables us to account for latent dependencies, which is another prevalent feature of the NFT market, as participants often transition between the roles of buyers and sellers.

We incorporate two types of network measures in our empirical setting: (i) the network of past transactions, which gauges the trading experience and the information it brings to the auction about market value and reputation; and (ii) platform-based connections, measuring popularity. Our analysis indicates that while the trading network of sellers is critically important across the auction price distribution, its impact appears to decline as prices increase. Platform followers are less essential for buyers but serve as a conduit for the popularity of sellers, particularly impacting the most expensive NFTs. Even within decentralized markets, our findings highlight the significant influence of trading networks and platform followers, especially for sellers of the most expensive NFTs.

Our contribution to the empirical literature on networks and decision making lies in our study of factors that influence price formation. We focus on NFTs for digital art, extending the foundations laid by previous studies, to go beyond the investigation of data patterns using aggregate statistics, hedonic regressions, visualization, and machine learning techniques (e.g., Nadini et al. 2021, Vasan et al. 2022 and Alizadeh et al. 2023). Our work threads together two strands of literature on traditional art auctions (e.g., Ashenfelter and Graddy 2003, Beggs and Graddy 2009, Botelho and Gertsberg 2022, De Silva et al. 2022a and De Silva et al. 2022b) and the influence of platform connections on market outcomes (e.g., Etter et al. 2019 and Grover et al. 2022), by introducing a network dimension into bidding decisions and ultimately the price determination process. Finally, our paper complements the work by Oh et al. (2022a), which assesses investor performance in the NFT market with an emphasis on experience. While a broad network often suggests substantial experience, our research focuses on understanding the distinct effects of the network structure and platform reputation across the entire range of prices.

The remainder of the paper is organized as follows. In Section 1.1, we present information on CryptoArt and the Foundation platform. In Section 1.2, we explore theoretical predictions. Section 1.3 describes the auction data on the Blockchain. Sections 1.4 and 1.5 present an empirical investigation of the impact of trading networks and platform connections on auction prices. Finally, in Section 1.6, we conclude our study, summarizing findings and discussing implications for the digital art market.

1.1 CryptoArt and the Foundation Platform

During the initial stages of blockchain technology, value transfer primarily relied on fungible tokens (FT), like Bitcoin and Ethereum. These tokens possess traits of homogeneity, interchangeability, divisibility, and replaceability. Blockchain users later found new applications for the technology to verify digital assets. Digital assets are distinct entities that are non-interchangeable. This led to the emergence of Non-Fungible Tokens (NFT) to address the requirement for recording singular, verifiable, and non-interchangeable assets on the blockchain.

NFTs encompass various categories, including Collectibles, Gaming, Metaverses, Utilities, and CryptoArt. CryptoArt provides artists with an alternative avenue to sell their creations, facilitated by specialized art platforms that support various transaction formats, including auctions. Owning such an NFT is akin to possessing a digital certificate of authenticity for the associated artwork, making it valuable as a verifiable and tradable good (Oh et al., 2022a). An important distinction from traditional art is that digital art sold as an NFT is almost exclusively sought after for its market value. Personal enjoyment of digital art can be achieved simply by downloading it at no cost and at the same quality as enjoyed by its owner. In other words, its consumption lacks the exclusivity of traditional art. Yet, what remains exclusive are the ownership bragging rights and the ability to resell. Drawing on Becker's earlier work on social influence and pricing (Becker, 1991), consumer demand can be strongly influenced by social factors and perceptions of desirability within a community. Becker's model of restaurant pricing highlights how social interactions shape consumer preferences and behaviors, underscoring the importance of incorporating such dynamics into economic models. Recent research by Oh et al. 2023 on NFT "generative" collections sheds light on pricing patterns, revealing shifts in demand driven by market sentiment and social dynamics, rather than solely intrinsic value.[1]

Although CryptoArt operates mainly on the Ethereum blockchain, its market dynamics

[1] This study emphasizes differences between the primary and secondary market outcomes for "generative" collections in contrast to our research which focuses on primary sales of all CryptoArt. These collections are unique and present variations of the same object or theme.

are not solely tethered to the value of Ether (ETH) (Dowling, 2022). Figure 1.1 aggregates information from all transactions of CryptoArt available on the Foundation platform from February 5, 2021 to December 5, 2022 and illustrates that the transaction values are closely correlated in both USD and ETH, with exceptions during the period of steady cryptocurrency market decline that started at the end of 2021.[2]

Figure 1.1: Number of NFT auctions and prices over time

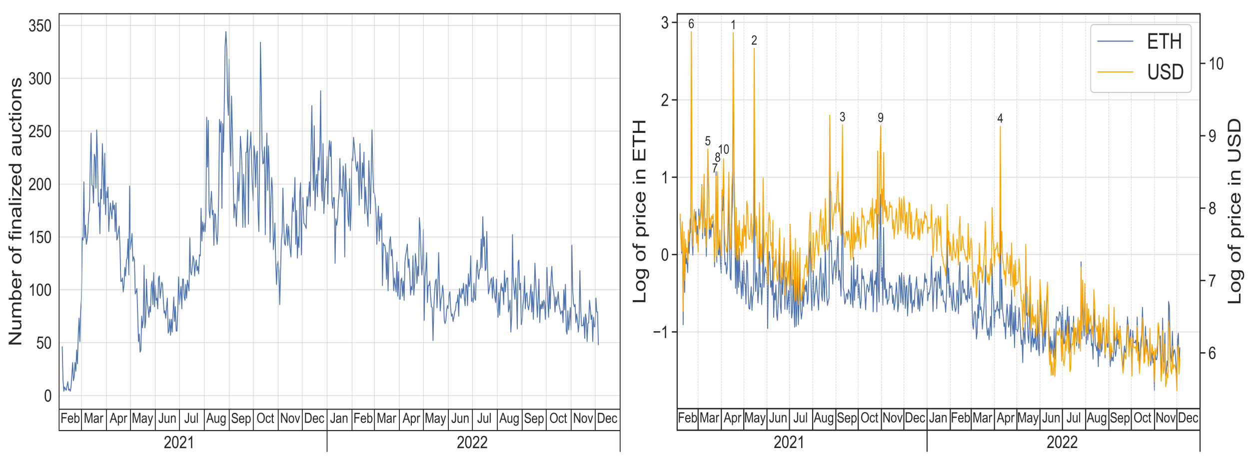

Notes: The figure on the left presents the daily total number of auctions. The figure on the right shows the daily average transaction prices in Ethereum and their corresponding value in USD. It also identifies the timing of sales for the top ten most expensive NFTs, with additional information delegated to Table A1.1.

Several marketplaces, including SuperRare and OpenSea, offer platforms for CryptoArt. However, Foundation distinguishes itself as a platform solely dedicated to the sales of CryptoArt, setting it apart from others that cater to a broader spectrum of categories. Foundation has an invitation-based model that allows any user with an invitation to join the market, eliminating the need for evaluation by a select group. Launched in February

[2]In November 2022, FTX, a prominent exchange with a total value of $32 billion, declared bankruptcy following a cryptocurrency market scenario similar to a bank run. This event had a ripple effect across the entire cryptocurrency market, leading to a 75% decline in the value of Bitcoin, the largest cryptocurrency, from its 2021 peak. This incident differed from other cryptocurrency crashes in 2022, like those of LUNA and TerraUSD, as it significantly eroded market security and trust (Yaffe-Bellany, 2022).

2021, the Foundation remains a prominent platform in the CryptoArt domain. Like most markets, it experienced an initial surge in daily auctions but later stabilized at around 100 daily auctions, as depicted in Figure 1.1.[3]

Upon joining the marketplace, users can mint new NFTs, enabling them to sell their creations directly to interested buyers. Artists upload their work along with a name and description to the platform, where it is registered on the blockchain via a smart contract[4] linked to their wallet.[5] The ERC-721 standard on Ethereum outlines the separation of NFT object data and proof of ownership. Each wallet is equipped with a public address, which is accessible to anyone, and a private key that remains exclusive to the wallet's owner. The key is necessary for executing cryptocurrency transactions. The minting process involves choosing a marketplace, creating a crypto wallet, inputting metadata, and listing the NFT for sale, rendering it a decentralized process devoid of intermediaries. Ownership is recorded on the blockchain's distributed ledger but does not grant copyright or intellectual property rights to the underlying content. Whenever the NFT changes hands within the platform, the seller pays a percentage of subsequent sales (royalties) to the original creator.

An NFT can be listed for sale when the owner specifies a "Buy Now" value for immediate purchase or sets a reserve price for auction. The auction starts when a bidder submits a bid at the reservation price and concludes 24 hours subsequent to the initial bid.[6] The owner

[3]Despite market fluctuations affecting all categories of NFTs, the art and collectible segment experienced the least impact, according to the February 2024 report from NonFungible.com. Activity within this segment has remained relatively stable over the past year, with monthly transactions averaging around 1 million USD.

[4]"A smart contract is simply a program that runs on the Ethereum blockchain. It's a collection of code (its functions) and data (its state) that resides at a specific address on the Ethereum blockchain." See Ethereum Development Documentation for more details.

[5]Foundation currently supports wallets provided by MetaMask, Coinbase, and those compatible with WalletConnect. While various types of crypto wallets can store both ETH and NFTs with limited owner information, exchanging them requires the use of a crypto exchange like Coinbase. Using Coinbase necessitates providing personal information such as social security number. Fraud detection mechanisms include algorithms that monitor IPs, accounts, transactions, and user reports to flag transaction that are not done according to policy and help minimize the possibility of wash trades and fraud.

[6]At any given time, an auction can be in one of four possible states. An open auction refers to an ongoing

of the NFT holds the authority to modify the reservation price only before the first bid is submitted. Upon the conclusion of the auction, the highest bidders, who becomes the auction winner, transfers a sum matching their bid to the seller's wallet and the NFT is transferred.[7] A listed NFT cannot be transferred to a different account or burned.[8]

The Foundation also functions as a social network, permitting users to follow profiles of their choice. Over time, creators can build reputation through the sale of art pieces that appreciate in value, while collectors can form networks based on their prior acquisitions. As the user base and artwork sales increase, the network's structure changes.

As a new market, Foundation underwent significant transformations. During its rise, which stretched from February 2021 to September 2021, the market saw rapid growth characterized by numerous daily auctions and high volatility, as shown in Figure 1.1. However, from September 2021 to April 2022, the increase in the number of auctions plateaued, indicating the end of rapid growth in numbers and the attainment of maturity. This phase coincided with the peak of Ethereum exchange rates. Subsequently, from April 2022 to December 2022, a period that aligned with the cryptocurrency market crash, the number of auctions experienced a decline and eventually stabilized with reduced volatility.[9]

As implied by the right panel of Figure 1.1, the price of some NFTs reached into millions of dollars. This is more precisely documented in Table A1.1, which presents prices of the

auction that has not been canceled or finalized yet. Such an auction may be either active and still accepting bids or pending finalization. On the other hand, a canceled auction indicates that it was terminated before reaching the reserve price. An invalidated auction is one that has been rendered invalid due to another action, such as a Buy Now option being exercised. Finally, a finalized auction signifies that the auction process has been completed, and the NFT has been successfully transferred to the winning bidder.

[7] Over time, Foundation has introduced various alternative methods for selling NFTs. In addition to auctions, these methods include Buy Now, Offers, Drops, Editions, Worlds, and Batch Listing. For more detailed information on these alternative selling methods, please refer to the Foundation Help Center.

[8] Burning is the irreversible destruction of an NFT by sending it to a designated burn address. This action renders the NFT unusable and is commonly used to decrease the total number of tokens available.

[9] The price of Ethereum surged to $4,644 in mid-November 2021, reached its lowest value at $993 in mid-June 2022, and has been steadily recovering since then, reaching $2,920 today (on February 21, 2024).

ten most expensive NFTs in the sample. Leading this list is “Stay Free,” which sold for $5.1 million, surpassing the sale prices of notable artworks like Claude Monet’s “Vernon Soleil”, which sold for $4.7 million at Sotheby’s in June of this year, and “Paysage, environs du Havre”, which fetched $402 thousand in March 2021, around the time of the NFT’s sale. “Stay Free” sold for nearly five times the price of Pablo Picasso’s “Tête de femme”, which recently sold at the same auction house. Despite the digital nature of cryptoart, which is widely accessible to anyone with internet access, their prices often reach levels typically associated with works by the most renowned painters.

1.2 Conceptual Framework

This section offers a conceptual framework that sets the stage for the expectations concerning the subsequent empirical analysis. In any time period t, n individuals are actively participating in an NFT auction. The expected value of the NFT i for a buyer a depends on various factors, including a privately observed signal, NFT characteristics, the seller’s identity and reputation, the network of buyer a at time $t-1$ and the number of followers and users followed on the Foundation platform. Let the vector of variables $\boldsymbol{w}_{ait}$ include all those characteristics with the NFT value estimate for bidder a represented by $Z_{ait} = f(\boldsymbol{w}_{ait})$. Let Ω_{n-2} be the information that is revealed during the auction process through the dropout prices of other participants at the beginning of the last round of bids. The auction format employed by the Foundation is an asymmetric variant of the auction framework described by Milgrom and Weber (1982). The asymmetric version was introduced by Wilson (1998) and subsequently generalized by Hong and Shum (2003) to encompass both common and private value frameworks. Assuming that the expected value of an NFT is strictly increasing in the value estimates of individual bidders (a typical assumption in the literature) then the theory predicts that equilibrium prices will also experience an increase as a direct consequence of the bidders' estimates.

Let $\beta_{(n-1)}$ denote the $(n-1)$-th order statistic of all bids excluding that of buyer a. The price P paid by buyer a in a Bayesian–Nash Equilibrium of the asymmetric English auction is:

$$P_a = E(V_{it}|Z_{ait}; \beta_a(Z_{ait}) = \beta_{(n-1)}; \Omega_{n-2}),$$

which is increasing in the value estimates. This follows from Proposition 1 in Hong and Shum (2003). Note that, the relationship between the value estimates and the vector encompassing observables for bidder a outside of the auction process, namely $Z_{ait} = f(\boldsymbol{w}_{ait})$, implies that those characteristics can potentially influence prices asymmetrically across the distribution. In our case, connections through networks and platforms may lead to asymmetric information among bidders. A few inferences can be made based on existing works in the auction literature: 1) **Access to more information drives aggressive bidding behavior.** According to Theorem 12 in Milgrom and Weber (1982), bidders with greater access to information, face less uncertainty about the market value of the item under auction and tend to bid more aggressively.[10] We view trading networks as conduits for information transmission about the market value of NFTs. The presence of a bidder with a significant trading network signals higher market value. Likewise, the presence of a seller with significant network is a signal of solid reputation adding value to the artwork on sale. If trading networks or platform connections carry information to bidders, we would expect to see a positive impact on the price. 2) **Large platform following influences bidding behavior.** Bidders with large following wield disproportionate influence that affects the perception of market value; their presence may lead to systematic shift in the perceived distribution of values of followers

[10]Note that Hong and Shum (2003) provide an example of a parametric family of distributions where the equilibrium bidding functions have closed-form solutions. In this example, bidder valuations follow a log-normal distribution, and more information leads to differential information rents in a common value context.

inducing more aggressive bidding behavior (see Proposition 3.3 in Maskin and Riley (2000) and De Silva et al. (2003) on the implications of those asymmetries).

Figure 1.2: Network structures with interdependence

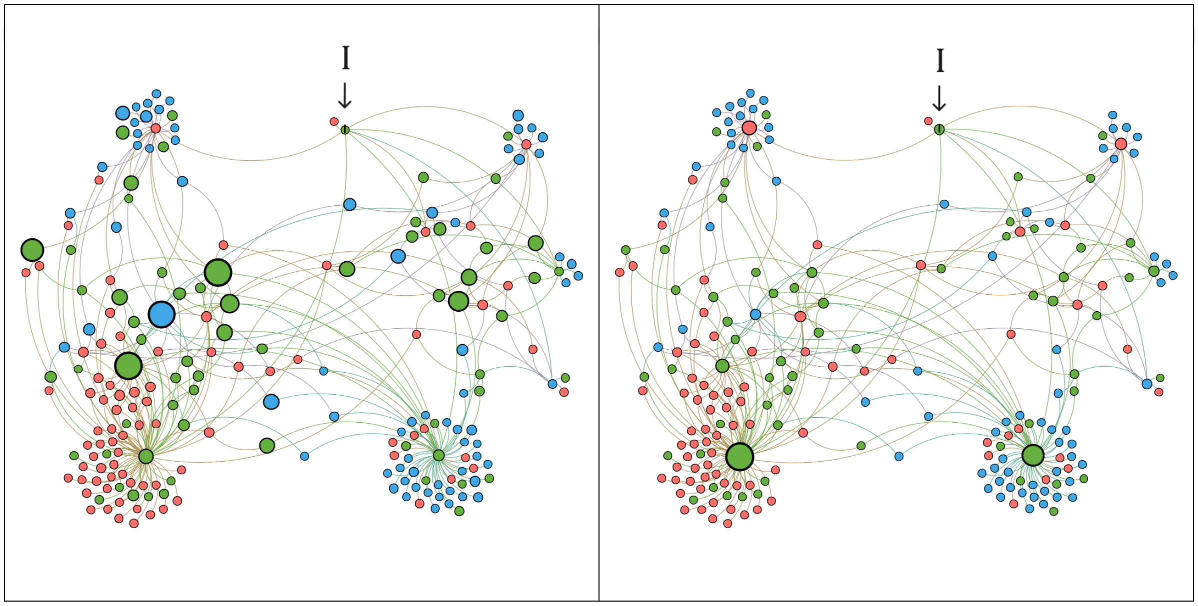

Notes: The network structure of a representative auction participant, denoted as I, over our sample period, featuring a walk of length 2. Nodes shaded in green depict users who engaged both in buying and selling activities. Red nodes represent sellers, while blue nodes represent buyers. In the figure to the right, the size of each node is proportional to its Katz centrality and in the figure to the left it is proportional to the number of followers on the platform.

While the theory underscores the critical impact of asymmetries on market outcomes, a practical question arises regarding the prevalence of networked bidders who can influence bidding behavior in NFT auctions. Figure 1.2 sheds light on this issue by showing a snapshot of the trading network structure for a representative auction participant from our sample, labeled *I*. In this figure, red nodes represent sellers, blue nodes represent buyers, and green nodes represent auction participants who engaged both in buying and selling. The size of the node is proportional to the number of trading connections (left panel) or the number of followers on the platform (right panel).

Judging by the size of each node, the figure reveals that while participant I may not be a well connected or popular trader, she is facing some competitors with denser trading networks or larger number of followers who in turn are competing against other well-connected platform participants. Moreover, the evidence brings out an additional layer of complexity. Individuals involved in transactions, particularly those transitioning from buyers to sellers and vice versa, can create interdependence across networks. For instance, a popular buyer could sell an NFT whose high price might not be determined by her trading network but instead her popularity as a buyer. This naturally affects bidding behavior and could potentially introduce estimation biases if these latent dependencies are not controlled for.

1.3 Auction Data on the Blockchain

Our primary data source consists of the auctions conducted on the Foundation platform from February 5, 2021, to December 5, 2022. Foundation utilizes Ethereum as its native currency, and all transactions are recorded using smart contracts on the Ethereum blockchain. An important feature of this dataset is that due to the comprehensive ledger maintained on the blockchain, we can access not only the details of an auction and its corresponding NFT but also the past activities of all participants. This includes other sales by the sellers and purchases by the buyers. Additionally, the unique identification of users through distinct addresses allows us to trace their social interactions within the Foundation platform.

1.3.1 Descriptive Statistics

To obtain the relevant data, we accessed the subgraph hosted by the Foundation platform on thegraph.com; thegraph.com is a decentralized protocol specifically designed for indexing and querying blockchain data. We selected the finalized auctions, to focus on completed transactions. The auction information includes the time that the auction is created, the reservation price, the history of reservation price changes if applicable, and information about bidders and the amount of their bid. After eliminating auctions involving participants banned or suspended from the platform due to terms of service violations, the remaining count totals 89,385 auctions.[11] We also excluded resales, a category distinct from auctions initiated by creators and currently less prevalent on the Foundation platform, resulting in a final count of 86,989 auctions.

Panel A of Table 1.1 provides auction summary statistics for the period of analysis. The average winning bid in auctions stands at 0.70 ETH, with a median of 0.30 ETH. The average duration between listing and final sale is roughly 28 days; however, half of the NFTs in our data set found a buyer within just four days of their initial listing. This listing-to-sale duration provides a more realistic assessment of the time it took for the seller to successfully organize a sale of an NFT compared to the 24-hour auction duration, particularly in cases of pre-sale auctions or auctions where the owner changed the reservation price.[12]

One attribute shared by participants in the Foundation's auctions with those in online marketplaces and the stock exchange, is their capacity to assume multiple roles. In contrast, traditional art auctions mostly involve a one-directional flow of primary sales, where artists create pieces subsequently sold by auction houses and acquired by collectors, often by art dealers (De Silva et al., 2022a), with very limited overlap between the groups of buyers and sellers. This one-way transactional feature is also shared by government procurement auctions

[11] Penalties for any form of misrepresentation on the platform include account termination and referral to law enforcement.

[12] Pre-sale auctions are relatively infrequent. Some *Fixed Pricing Drops* may have a pre-sale phase, exclusively accessible to chosen collectors as designated by the seller. For more information, please refer to the Foundation Help Center.

Table 1.1: Descriptive Statistics

Variable	Mean	Deviation Standard	Min	Max	Number of Observations
		A. Auction Characteristics			
Winning Bid Amount	0.703	8.618	0.050	2224.000	86989
Listing-to-Sale duration (Hours)	675.797	1359.979	23.013	14226.608	86989
Reservation Price Change	0.220	0.414	0.000	1.000	86989
		B. Participants Type in Auctions			
No. of Bidders Never Won	0.125	0.633	0.000	24.000	86989
No. of Artist and Seller	1.048	1.104	0.000	15.000	86989
No. of Artist and Collector	1.665	1.921	0.000	39.000	86989
No. of Collector	2.566	2.216	0.000	34.000	86989
Seller is DAO	0.003	0.057	0.000	1.000	86989
Buyer is DAO	0.004	0.065	0.000	1.000	86989
		C. NFT characteristics			
Length of NFT's Description	232.975	228.232	0.000	1000.000	86988
Still Image	0.653	0.476	0.000	1.000	86989
Animated	0.340	0.474	0.000	1.000	86989
3D Format	0.007	0.082	0.000	1.000	86989
		D. Network and Social Media			
Centrality Seller	0.012	0.055	0.000	1.000	85579
Centrality Buyer	0.077	0.214	0.000	1.000	82101
Centrality 2nd Highest Bidder	0.042	0.129	0.000	1.000	20540
Number of Followers Seller	704.268	1024.362	0.000	14100.000	86987
Number of Following Seller	375.387	2283.088	0.000	161000.000	86987
Number of Followers Buyer	1818.031	2657.301	0.000	14000.000	86979
Number of Following Buyer	233.959	815.123	0.000	101100.000	86979
Seller Has Twitter	0.957	0.202	0.000	1.000	86987
Seller Has Instagram	0.746	0.435	0.000	1.000	86987
Buyer Has Twitter	0.672	0.470	0.000	1.000	86979
Buyer Has Instagram	0.303	0.460	0.000	1.000	86979

Notes: DAO stands for Decentralized Autonomous Organization, and the computation of Katz centrality follows the method outlined in Section 1.3.2. The participant types in Panel B are determined based on the categories illustrated in Figure 1.3.

(Hortaçsu and Perrigne, 2021). However, due to the decentralized nature of NFT markets, the accessibility of information, simplified transactions, and the absence of intermediaries like art dealers, creators have ample opportunities to participate in auctions as bidders.

Therefore, we categorize users into four groups based on their past activities within the platform. A seller refers to a user who has successfully sold an NFT, while a collector denotes a user who was the winner in an auction. An artist represents a creator who has minted an NFT, and a bidder is a user who has participated in auctions by placing bids, regardless of winning.

Our sample is restricted to primary auction sales on the Foundation platform excluding resale opportunities, that resulted in 46,195 unique users. It is important to note that a user can assume multiple roles on the platform. For instance, approximately 28 percent of the NFT creators within our sample engaged as bidders in auctions, and roughly 19 percent of collectors have minted and sold their own NFTs. About 10% of all unique users have had experiences in all listed categories, while all but three artists sold their own work directly in the market. These categories and their sizes are visually illustrated in Figure 1.3 and summary statistics detailing the participant types in auctions are presented in Panel B of Table 1.1.[13]

We also obtained information for each NFT, including the creator's unique identifier on the blockchain, the mint date, and the IPFS path which allows us to locate the NFT's metadata.[14] Subsequently, using the previously acquired addresses, we retrieved the metadata

[13]In addition, we identified Decentralized Autonomous Organizations (DAO) in our data. DAOs are blockchain-based entities that operate without centralized control or management. They are designed to be autonomous and self-governing, relying on smart contracts and code to execute decisions and manage resources. DAOs can curate and manage collections of digital art and have the ability to pool funds from members to collectively purchase high-value NFTs, enabling broader ownership or shared access. Overall, we observed 48 DAOs in our data with participation in 381 auctions, which represents less than 1 percent of the total number of NFT auctions.

[14]InterPlanetary File System (IPFS) is a decentralized file storage protocol employed for storing NFT-related

Figure 1.3: Type of participants in Auctions

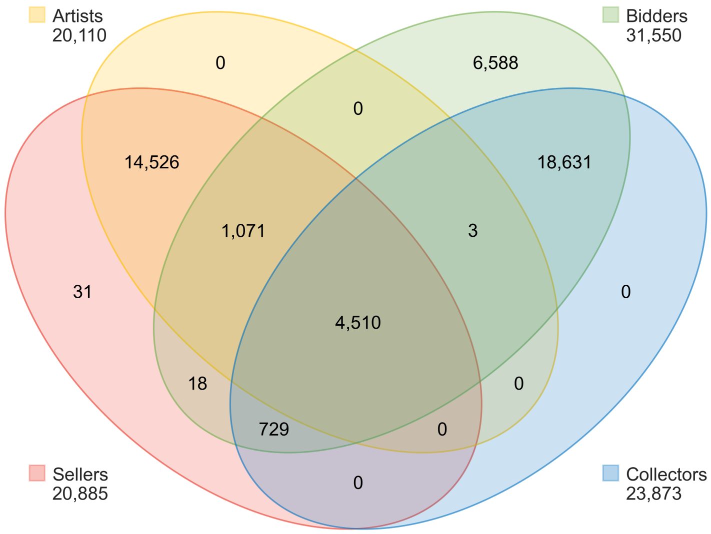

Note: This Venn type diagram shows the number of participants in the auctions by type. An artist is a participant who creates NFTs. Sellers are defined as participants who sell NFTs. Bidders are participants who placed bids in an auction, and collectors (or buyers) are the participants who won at least one auction.

for each individual NFT from ipfs.tech. This metadata contains information on the NFTs such as name, description, and the link to the stored file. We utilized the link to extract both the file name and its corresponding extension, which in turn allows us to identify the specific file type.

To categorize the file types, we classified them into three distinct groups. Files with extensions ".jpg," ".png," and ".svg" are classified as static, indicating non-animated or still images. Files with extensions ".gif", ".mov", and ".mp4" are categorized as animated. Additionally, 3D images are identified by file formats such as ".glb" or ".gltf". Creators can also add more details to NFTs by writing descriptions, which consist of around 229 characters on average. More specific characteristics of the NFTs are listed in Panel C of Table 1.1.

We employed users' unique blockchain identification to access their profiles on the Foun-

data. For further information, please visit ipfs.tech.

dation website. User-related information for all participants in auctions was directly obtained from the Foundation.app website. On this platform, users can follow other accounts of interest, allowing us to observe the number of followers and accounts they follow. Buyers tend to have more followers and follow fewer users compared to sellers. On average, buyers have around 1,818 followers, which is 2.6 times higher than sellers. They also follow approximately 234 accounts, which is 0.62 times the number followed by sellers.

Users have the option to customize their accounts by linking external websites and integrating social media platforms, with the Foundation website design prominently featuring Twitter and Instagram accounts. The majority of creators (95 percent) have linked their Twitter accounts to the platform, while a substantial portion (74 percent) have linked their Instagram accounts. In contrast, fewer buyers have linked their Twitter accounts (68 percent), and even fewer have connected their Instagram accounts (30 percent). The specifics of user social media activities are provided in Panel D of Table 1.1.

Users create the network through their prior transactions. Using the methodology detailed in section 1.3.2, we calculated Katz centrality for all users, providing a measure of the relative importance of each user trading in past auctions. Summary statistics for these values in our auction data can be found in Panel D of Table 1.1.

Lastly, we obtained the exchange rate of Ethereum (ETH) to USD from etherscan.io, a widely-used source for tracking the Ethereum-to-US-dollar exchange rate. Before we introduce the empirical evidence based on the variables described above, we detail below the construction of the network measures.

1.3.2 Network Measures

We construct the network based on past transactions where nodes in the network represent users involved in NFT sales or purchases (Kranton and Minehart, 2001). An edge in the network represents a connection from the seller to the buyer and is weighted by the winning bid. The weight of each edge corresponds to the value of transactions in ETH. We use Katz centrality to measure the centrality of each node k at time t using the following formula:

$$kc_{k,t}(N_t) = \sum_l \sum_j \delta^l \mathbf{A}^l_{t,k,j}, \tag{1.1}$$

where N_t represents the network of sellers and buyers spanning transactions from the last 30 days, but excluding those at t, with $\mathbf{A}_t$ representing its corresponding adjacency matrix. A non-zero value of $\mathbf{A}_{t,k,j}$ indicates the presence of an edge between node k and j during the time frame before t, while a zero value of $\mathbf{A}_{t,k,j}$ signifies the absence of such an edge within the same time frame. The index l denotes the length of walks emanating from node k and δ represents the discount factor. Following standard practice (Bloch et al., 2023), the discount factor is determined by establishing an upper bound based on the maximum eigenvalue of matrix $\mathbf{A}_t$.[15] Katz centrality allows us to assess the importance of nodes within a trading network. It extends the concept of eigenvector centrality and takes into account not only a node's direct connections but also its indirect connections through other nodes in the network.

Figure 1.4 provides a way to visualize trading networks of sellers and buyers of digital art NFTs. It illustrates the 300 highest-value transactions per period, during three distinct

[15]To ensure convergence, for all t, δ need to satisfy $\delta < \lambda_t^{-1}$, where λ_t is the largest eigenvalue of N_t. We computed the largest eigenvalue for each t, with the maximum of these values being $2,280$. We selected δ corresponding to a larger eigenvalue of approximately 2,500. We later employed min-max normalization to ensure comparability across different days, accounting for the growing number of network nodes over time.

Figure 1.4: The top 300 highest-value transactions

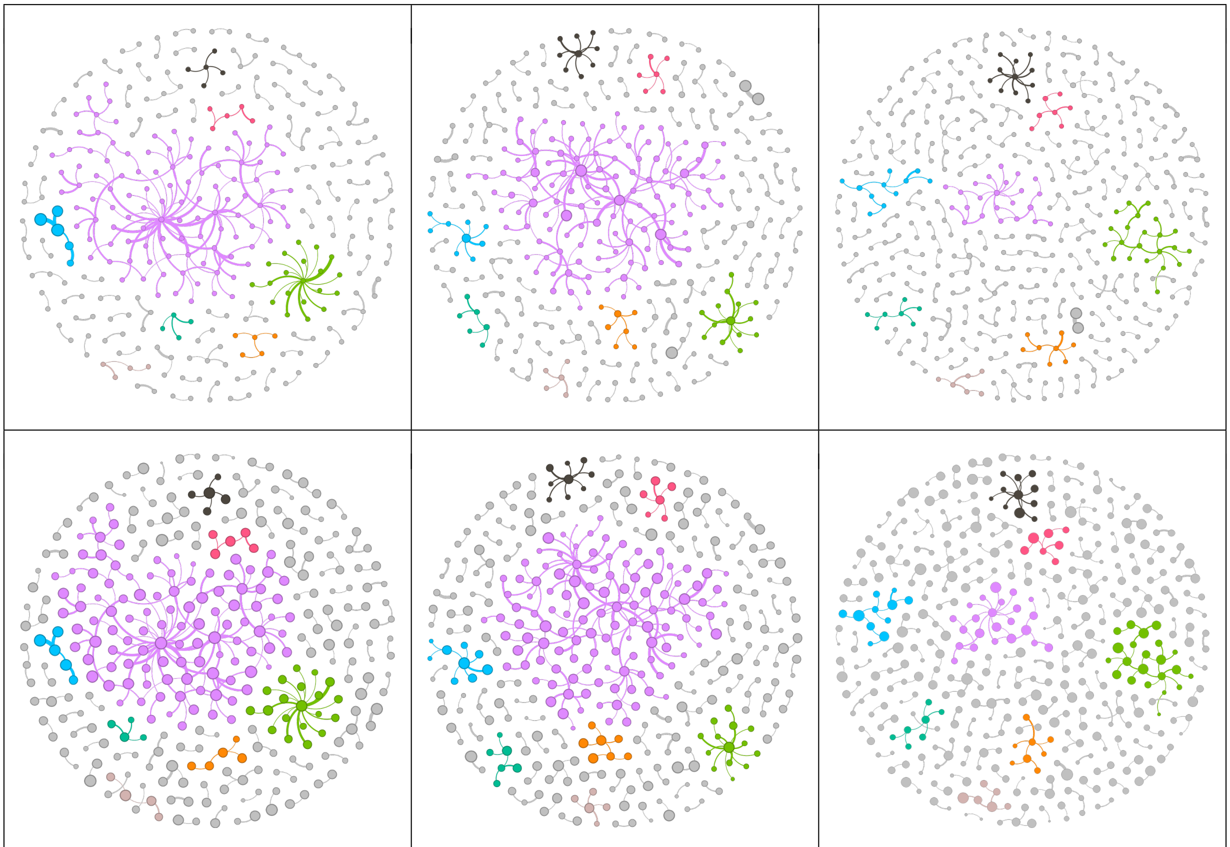

Rise	Maturity	Decline

Notes: The “Rise” period spans from February 5, 2021, to September 1, 2021, while the “Maturity” phase extends from September 1, 2021, to April 1, 2022. The “Decline” period is from April 1, 2022, to December 5, 2022. The thickness of edges denotes the transaction value in ETH. In the top row, node size corresponds to Katz centrality, while in the bottom row, node size indicates the number of followers. Connected components are highlighted.

phases of the market: the rise, maturity, and decline. This sample represents approximately 1% of the transactions per period, a size large enough to provide a clear visualization of the network structure but not too large to obstruct visual clarity. In these network graphs, the nodes represent participants identified as sellers or buyers, and the edges are links whose thickness varies by the value of user transactions. In the top row, node size signifies Katz centrality for the specified period as in equation (1.1), capturing the relative importance of nodes within the NFT trading network. In the bottom row, node size reflects the number of followers. Connected components are highlighted, showing the auction participants who are linked through some transaction.

In the first phase, the top 300 highest-value transactions were primarily concentrated within a large connected component featuring a small number of highly central nodes. However, dominant nodes and transactions gradually lost their prominence as the market transitioned from the phase of maturity to the decline. In the right panels, we see that participants involved in the most expensive transactions are not all interconnected, while their transactions become less central to the network's structure. The figure also reveals that for the most expensive NFTs, follower connections are more prominent than the trading network. Conversely, the relative importance of the trading network increases for the lowest priced NFTs.[16]

[16] These figures are available by the authors upon request.

1.4 Networks and Platforms Influence on NFT Prices

This section presents a series of basic regressions aimed at exploring the impact of trading and social networks, as a conduit of information, on prices. We estimate the following equation:

$$y_{iast} = \boldsymbol{N}'_{iast}\boldsymbol{\delta}_1 + \boldsymbol{F}'_{iast}\boldsymbol{\delta}_2 + \boldsymbol{W}'_{iast}\boldsymbol{\theta} + f_d(D_{it}) + f_e(E_t) + \alpha_a + \alpha_s + \mu_t + u_{iast}, \tag{1.2}$$

where y_{iast} denotes the logarithm of the winning bid in an NFT auction i bought by buyer a, and sold by seller s at time t. The vector $\boldsymbol{N}_{iast}$ denotes network variables and $\boldsymbol{F}_{iast}$ includes the number of accounts in the Foundation following buyers and sellers, and the number of accounts the buyer or the seller follows. The variable $\boldsymbol{W}_{iast} = (\boldsymbol{S}'_{iast}, \boldsymbol{B}'_{it}, \boldsymbol{X}'_i)'$ are control variables. The vector $\boldsymbol{S}_{iast}$ includes indicators for social media presence (i.e, the buyer has a Twitter or Instagram account connected to the Foundation platform), $\boldsymbol{B}_{it}$ are auction-related controls, including bidder type and an indicator denoting changes in the reservation price, $\boldsymbol{X}_i$ are NFT related controls including the type of NFTs auctioned off and the length of their description, α_a is a buyer effect, α_s is a seller effect, μ_t are time dummies and u_{iast} is an error term. The model also includes two unknown functions in terms of the listing-to-sale duration of the auction D_{it} and the exchange rate E_t.[17] A detailed description of all the variables used in our analysis is provided in Table A1.2 in the appendix.

Auction participants can access information regarding the NFT's value in two distinct ways. First, they can utilize past connections ($\boldsymbol{N}$), quantified by the Katz centrality of the seller, the buyer and the second highest bidder. This metric allows us to gauge experience that conveys information about the market value; a higher centrality score for the seller indicates extensive trading experience and a strong reputation through associations with

[17] The functions f_e and f_d are estimated using cubic B-spline functions with five knots

important users. Similarly, a high centrality score for a buyer suggests robust trading network connections that can reduce uncertainty in the value of a trade.[18] Second, participants can assess the popularity of sellers and buyers by examining the number of followers and profiles they follow within the Foundation platform ($\boldsymbol{F}$). We transform the variables and consider the logarithm of the number of followers and number of profiles followed. Foundation allows for asymmetric relationships, where a user can follow a profile without requiring confirmation from the profile being followed. In such relationships, a buyer's decision, for example, to follow another profile typically signifies an interest in obtaining information about that profile's activities which can lead to more informed decisions and lower prices.[19] The number of followers serves as a measure of influence on the platform, indicating that others seek information from those they follow. Users with a higher number of followers on platforms are generally considered more popular, as more users express interest in obtaining information by following their accounts, a concept well-documented in the literature (Grover et al., 2022; Kane et al., 2014).[20]

The first column of Table 1.2 presents Ordinary Least Squares (OLS) results. Columns (2), (3) and (4) present results obtained from estimating different variations of equation (1.2). Lastly, Column (5) shows results obtained by estimating the conditional mean model corresponding to equation (1.2). As expected, the results in the first column show that the network connections of the seller positively impact the winning bid. The influence of the

[18] Alizadeh et al. (2023) employ NFT data from the Moralis platform and presents an analysis of networks, shedding light on their structural characteristics, evolution, and interactions. The study reveals that a select group of buyers and sellers frequently engage in NFT sales and purchases, while the majority participate in a more limited number of transactions.

[19] According to Engelbrecht-Wiggans et al. (1983) and Hendricks and Porter (1988), bidders with superior information tend to achieve higher profit margins while paying lower prices compared to others.

[20] Participants can also gather information from external social media platforms, including Twitter and Instagram. In contrast to the Foundation platform, we lack direct data on the number of followers and accounts followed on Twitter and Instagram. We view these platforms as supplementary sources of information for participants.

Table 1.2: Regressions for the logarithm of winning bid

	(1)	(2)	(3)	(4)	(5)
Centrality Seller	0.675***	0.964***	1.061***	0.558***	0.598***
	(0.071)	(0.071)	(0.092)	(0.078)	(0.108)
Centrality Buyer	0.329***	0.377***	0.120**	0.428***	0.175***
	(0.042)	(0.041)	(0.059)	(0.037)	(0.058)
Centrality 2nd Highest Bidder	0.511***	0.590***	0.570***	0.405***	0.366***
	(0.043)	(0.043)	(0.047)	(0.039)	(0.048)
Number of Followers Seller	0.316***	0.288***	0.295***	0.384***	0.372***
	(0.006)	(0.006)	(0.008)	(0.051)	(0.068)
Number of Following Seller	−0.170***	−0.142***	−0.124***	−0.111**	−0.152**
	(0.004)	(0.004)	(0.005)	(0.045)	(0.059)
Number of Followers Buyer	0.210***	0.194***	0.122*	0.102***	−0.001
	(0.005)	(0.005)	(0.062)	(0.005)	(0.068)
Number of Following Buyer	−0.102***	−0.097***	−0.102*	−0.052***	0.020
	(0.004)	(0.004)	(0.054)	(0.004)	(0.056)
Auction Controls	Yes	Yes	Yes	Yes	Yes
NFT Controls	Yes	Yes	Yes	Yes	Yes
Social Media Variables	Yes	Yes	Yes	Yes	Yes
Semiparametric Functions	Yes	Yes	Yes	Yes	Yes
Month and Year Dummies	No	Yes	Yes	Yes	Yes
Buyer Effects	No	No	Yes	No	Yes
Seller Effects	No	No	No	Yes	Yes
Observations	18,103	18,103	18,103	18,103	18,103

Notes: The dependent variable is the logarithm of the winning bid in Ethereum for an NFT auction (i) sold by seller (s) and won by buyer (a) at time (t). Number of followers and following are logged. All models include a constant. Statistical significance levels are denoted as follows: *** indicates significance at the 1% level, ** at the 5% level, and * at the 10% level. Standard errors are enclosed in parentheses.

second highest bid, as a measure of competitive pressures, is also positive and significant, as expected. Moreover, it is interesting to see that while a higher number of followers positively influences the winning bid, a greater number of accounts followed has a negative impact. Previous work by Vasan et al. (2022) in the NFT-driven CryptoArt marketplace reveals that artists' success is influenced by perceived reputation and a follower base, leading to the formation of clusters driven by homophily that affect individual artists' achievements. Successful artists tend to attract repeated investments from a select group of collectors, highlighting the significance of artist-collector relationships in the digital art space.

The estimated effects of the centrality measure are attenuated in column (5), although they are still positive and significant at standard levels. Moreover, a higher number of followers for the seller continues to have a positive impact on the winning bid, while a higher number of accounts followed has a negative effect on the winning bid. In the case of buyers, the results in the last column suggest that the platform connections do not seem to differentially affect the average auction price paid by buyers.

As documented in the previous sections, the most expensive NFTs reached levels associated with artwork from celebrated artists. The results presented so far are not informative on this puzzling and understudied fact. In the next section, we go beyond classical regression analysis to address this issue.

1.5 Heterogeneous Effects across the Price Distribution

How do trading networks and platform connections affect low-priced and high-priced NFTs? In this section, we estimate the impact of these factors across the price distribution. Our empirical analysis offers several important findings. While trading networks remain critically important, their impact decreases across the distribution of NFT prices. Moreover, platform followers for sellers, possibly capturing popularity, help explain price differences among the highest NFT prices.

1.5.1 Methods

Before we present the results in the next section, it is convenient to introduce additional notation. Let the observed data be represented by $\{(y_{sa}, \boldsymbol{w}'_{sa}) : (s,a) \in \mathcal{D}\}$, where s denotes a seller and a denotes a buyer. The variable winning bid $y \in \mathcal{Y} \subseteq R$ is also indexed by auction i and time t as in equation (1.2), but we omit these indexes to simplify the notation. As above, let the vector of variables $\boldsymbol{w}$ include the vector of network variables, the number of accounts in the Foundation following buyers and those following sellers and the number of accounts the buyers or sellers follow, the indicator variables for social media presence, the auction specific controls, and the NFT related controls. All the models estimated below include controls for the listing-to-sale duration of the auction and the exchange rate, as well as individual time effects. Finally, let $P(\boldsymbol{w})$ denote a dictionary of transformations of $\boldsymbol{w}$ that includes B-splines functions for the listing-to-sale duration of the auction and the exchange rate as in equation (1.2).

Recent work by Chernozhukov et al. (2024) allows us to control for network and group dependencies that are latent and possibly correlated to the network variables.[21] Let $\alpha(v_s, y)$ and $\mu(v_a, y)$ denote seller and buyer latent heterogeneity, where v_s captures private information available to seller s. The variable v_a is defined similarly. We specify the conditional model as,

$$G_{y_{sa}}(y|\boldsymbol{w}_{sa}, v_s, v_a) = \Lambda_y \left(P(\boldsymbol{w}_{sa})' \boldsymbol{\gamma}(y) + \alpha(v_s, y) + \mu(v_a, y) \right), \tag{1.3}$$

[21] This approach can be valuable in addressing network effects due to latent linkages in our data, where buyers and sellers can assume multiple roles. For instance, the same pair of market participants, when their roles are reversed from seller to buyer and vice versa, may exhibit interdependence.

where $\Lambda_y(\cdot)$ is the logistic distribution and $\boldsymbol{\gamma}(y)$ is an unknown parameter that varies with the winning bid $y \in \mathcal{Y}$. The parameters in equation (1.3) are estimated by Maximum Likelihood (ML). As fixed effects in nonlinear models can lead to bias due to incidental parameters, it is advised to implement the bias corrections as in Fernández-Val and Weidner (2016).

Since y is continuous, the model stated in equation (1.3) is related to conditional panel quantile functions with individual intercepts. If we set $u_{sa} = G_{y_{sa}}(y|\boldsymbol{w}_{sa}, v_s, v_a)$, where $u_{sa}|\boldsymbol{w}_{sa}, v_s, v_a \sim \mathcal{U}(0,1)$, the τ-th quantile of y_{sa} conditional on $\boldsymbol{w}_{sa}$ is

$$Q_y(\tau|\boldsymbol{w}_{sa}) = \boldsymbol{w}'_{as}\boldsymbol{\gamma}(\tau) + \alpha_s(\tau) + \mu_a(\tau), \tag{1.4}$$

where $\tau \in (0,1)$ and $Q_y(\tau|\boldsymbol{w}_{sa})$ is the τ-th quantile of the conditional distribution of the winning bid y_{sa}, α_s is the seller effect, and μ_a denotes the buyer effect. Let the parameter vector be $\boldsymbol{\theta}(\tau) = (\boldsymbol{\gamma}(\tau)', \boldsymbol{\alpha}(\tau)', \boldsymbol{\mu}(\tau))' \in \boldsymbol{\Theta} \subseteq R^{p+n_a+n_s}$, where $\boldsymbol{\alpha}(\tau) = (\alpha_1(\tau), ..., \alpha_{n_s}(\tau))'$, and $\boldsymbol{\mu}(\tau) = (\mu_1(\tau), ..., \mu_{n_a}(\tau))'$. The following estimator is an extension of a one-way panel quantile estimator considered by Lamarche and Parker (2023):

$$\hat{\boldsymbol{\theta}}(\tau) = \underset{\boldsymbol{\theta} \in \boldsymbol{\Theta}}{\operatorname{argmin}} \sum_{(s,a) \in \mathcal{D}} \rho_\tau(y_{sa} - \boldsymbol{w}'_{sa}\boldsymbol{\gamma} - \alpha_s - \mu_a) + \lambda_1 \|\boldsymbol{\alpha}\|_1 + \lambda_2 \|\boldsymbol{\mu}\|_1, \tag{1.5}$$

where $\rho_\tau(u) = u(\tau - I(u < 0))$ is the quantile regression loss function and $\|\cdot\|_1$ denotes the ℓ_1 norm. The last two terms represent Lasso-type penalties with tuning parameters $(\lambda_1, \lambda_2) \geq 0$. Rather than using a bias correction formula to reduce the potential bias due to incidental parameters, the penalty terms in (1.5) help reduce the noise in the estimation of individual intercepts, and consequently, the penalized estimator can reduce the bias of the fixed effects estimator. The idea is related to Bester and Hansen (2009) who propose an approach to bias reduction in nonlinear models with fixed effects using a penalty function. The tuning parameters and the standard error of the estimator $\hat{\boldsymbol{\theta}}(\tau)$ are obtained following Lamarche and Parker (2023).

1.5.2 Main Results

We begin reporting panel quantile regression estimates, since the model can be efficiently estimated with a total of 13,052 seller and buyer effects and we expect distributional regressions and quantile regressions to deliver similar qualitative conclusions as shown in Table 1.3. In the next steps of this analysis, we are using Figure 1.5 and Figure 1.6 to present results for the main effects of interest included in the winning bid equation (1.4).

Figure 1.5 presents point estimates and 95 percent point-wise confidence intervals for the effect of trading networks across quantiles of the conditional distribution of winning bids. Buyers are depicted in blue, while sellers in red. The left panel shows results for the Katz centrality of the seller, and the middle panel shows results for the same measure constructed for the buyer. The panel on the right shows the estimated impact of the network of the bidder with the second highest bid.

It is interesting to see that trading networks do not seem to be as impactful at the highest trading prices. This is evident in the declining effect of seller centrality when moving across quantiles. While the seller's centrality is associated with higher prices at the upper tail of the distribution, they have a higher marginal impact at the lowest conditional quantiles.[22] Additionally, we observe a higher effect for the buyer's centrality in the lower tail, possibly implying that buyers with more trading connections in the past pay relatively more for low-priced NFTs. The effect of competition in the auctions, which is measured by the centrality of the second highest bidder, is positive and constant, consistent, once again, with

[22] As suggested by the figure, the slope coefficient is not significantly different across quantiles.

Figure 1.5: The effect of trading networks on winning bids

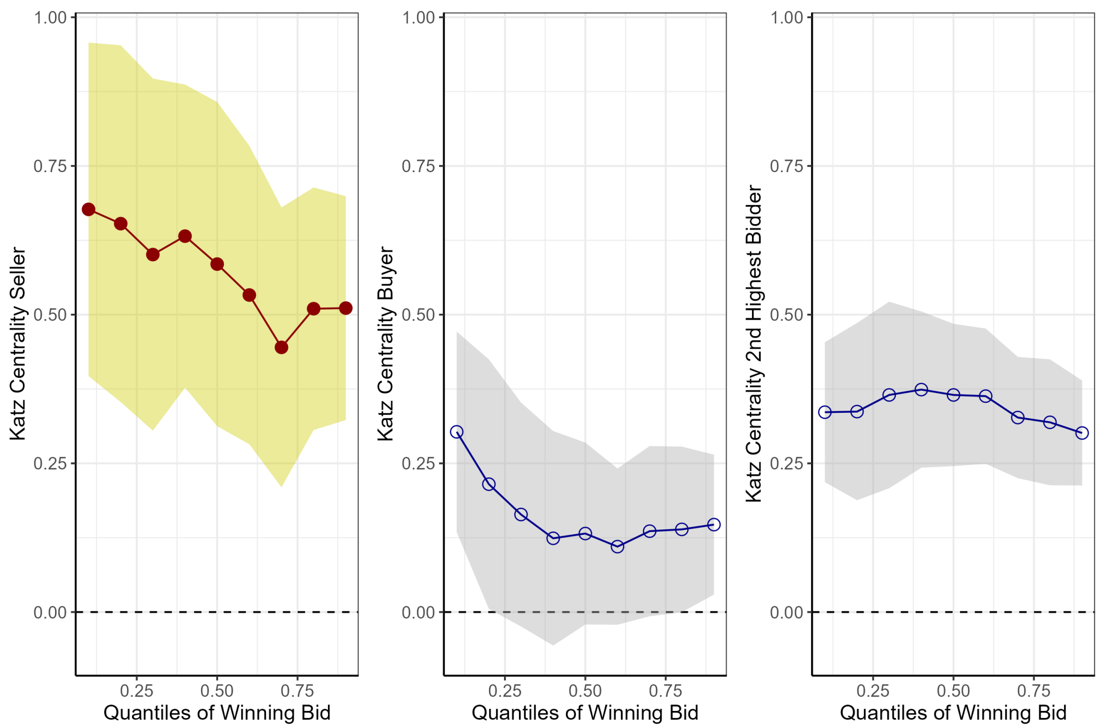

expectations.

Figure 1.6 displays the estimated effects of the logarithm of seller and buyer followers and the number of accounts followed as a function of the quantile τ of the conditional distribution of winning bids. Once again, the dotted line corresponds to the point estimate, while the shaded region represents a 95 percent point-wise confidence interval for these estimates. The results in the left panel reveal that, once we account for potential group dependencies, the impact of the number of followers of the buyers becomes consistently muted across quantiles. In contrast, the estimated effect of the number of followers of the seller is positive and increasing, suggesting that platform connectivity provides a channel through which influence and visibility might help explain conditionally high NFT prices.

The right panel of Figure 1.6 continues to show negligible and insignificant effects for the

Figure 1.6: The effect of platform connections on winning bids

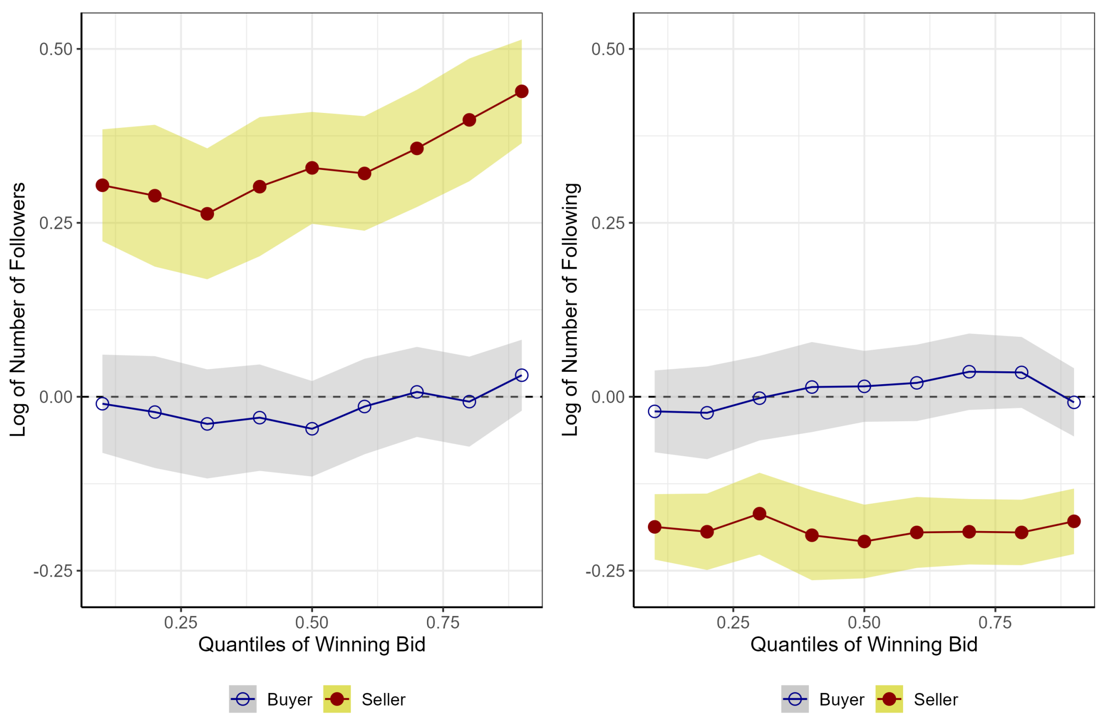

buyers, this time considering the number of accounts they follow. In contrast, the impact of the number of accounts followed by sellers is negative and constant across quantiles. The evidence seems to suggest that high trading prices might be associated with popular sellers who tend to lead and not follow other participants on the platform.

By comparing these results with the results shown in Table 1.2, we can gain additional insights in how platform connections affect price in the the digital art marketplace. For instance, in the first column of Table 1.2, we observe that the number of followers for both buyers and sellers exhibited a positive effect on winning bids, and the number of accounts followed had a negative effect. However, after controlling for seller and buyer effects in column (5), these patterns continue to hold only for followers of the seller. The quantile regression results in Figure 1.6 are qualitatively similar, but the estimated effects are 0.329 at the 0.5 quantile and 0.439 at the 0.9 quantile, representing an increase of roughly 33 percent and 19 percent with respect to the median and mean effects.

In summary, the results of this section suggest that controlling for latent interdependencies in the network is critical for estimating winning bid regressions in a digital art marketplace. We find that trading networks are relatively more influential in lower-priced NFTs. However, with high-priced NFTs, seller popularity has a more significant effect on the price even without relying on experience from past transactions. Notably, platform connections among sellers significantly impact the overall price distribution, particularly for higher-priced items.

1.5.3 Robustness to Modeling Unobserved Heterogeneity

Table 1.3 presents a comparison of estimates of panel quantile regressions and distributional regressions for the network variables. In this section, we estimate models with seller effects, as they appear to be the most important latent drivers of winning bids in the NFT auctions.

This is also convenient for the computational performance of the ML estimator, due to the demanding memory usage in models with a large number of sellers and buyers.[23] Nevertheless, we demonstrate that the results from the bias-corrected distributional regression with seller fixed effects closely align with those obtained through panel quantile regression. The model also includes Foundation variables and social media variables as in equation (1.2), but, due to the inclusion of seller effects, the effects are not always identified.

The first column of Table 1.3 present results obtained by panel quantile regression (PQR), and the next columns show results obtained by distributional regression estimators, with (BC) and without (DR) a bias correction. A direct comparison of the estimates can be made by noting that the signs of the coefficients in the distributional regression are opposite to those in the panel quantile regression. The table presents three panels (in columns) with results, and each panel provides estimates for quantiles $\{0.1, 0.5, 0.9\}$.

The results continue to suggest that trading networks provide greater informational advantages to sellers who sell at relatively lower prices, in comparison to those who sell at higher prices. While the point estimates do not show a sharp decline across quantiles, they do suggest that the seller's trading network may not remain the dominant driver of higher trading values of NFTs confirming the evidence provided in Figure 1.4. Based on the estimates, distributional regression results shows a decreasing effect for the seller's centrality across quantiles, a result similar to the one obtained by panel quantile regression. Lastly, the bias-corrected estimator of the distributional regression with seller fixed effects closely align with those of the panel quantile regression.

[23]Due to the estimation of more than 13,000 parameters in our application, the algorithm for ML with fixed effects encountered convergence issues.

Table 1.3: Results for Network Effects in Models with Seller Effects

	0.1 Quantile			0.5 Quantile			0.9 Quantile		
	PQR	DR	BC	PQR	DR	BC	PQR	DR	BC
Centrality Seller	0.482***	−3.675***	−2.451	0.492***	−3.075***	−2.394	0.351***	−1.835***	−1.274
	(0.126)	(1.407)		(0.101)	(1.083)		(0.1)	(0.57)	
Centrality Buyer	0.380***	−1.190*	−0.534	0.329***	−1.619***	−0.918	0.438***	−1.867***	−0.896
	(0.066)	(0.639)		(0.054)	(0.323)		(0.048)	(0.4)	
Centrality 2nd Highest Bidder	0.296***	−1.926***	−1.254	0.297***	−2.155***	−1.482	0.228***	−2.127***	−1.399
	(0.039)	(0.638)		(0.054)	(0.299)		(0.044)	(0.458)	
Number of Followers Buyer	0.047	−0.430	−0.275	0.073	−0.541	−0.388	0.090	−0.783	−0.502
	(0.007)	(0.058)		(0.006)	(0.040)		(0.006)	(0.078)	
Number of Following Buyer	−0.023	0.208	0.136	−0.037	0.255	0.181	−0.051	0.408	0.272
	(0.005)	(0.047)		(0.005)	(0.030)		(0.005)	(0.054)	
Foundation Variables	Yes	Yes	Yes	Yes	Yes	Yes	Yes	Yes	Yes
Social Media Variables	Yes	Yes	Yes	Yes	Yes	Yes	Yes	Yes	Yes
Auction Controls	Yes	Yes	Yes	Yes	Yes	Yes	Yes	Yes	Yes
NFT Controls	Yes	Yes	Yes	Yes	Yes	Yes	Yes	Yes	Yes
Semiparametric Functions	Yes	Yes	Yes	Yes	Yes	Yes	Yes	Yes	Yes
Monthly and Year Dummies	Yes	Yes	Yes	Yes	Yes	Yes	Yes	Yes	Yes
Seller Effects	Yes	Yes	Yes	Yes	Yes	Yes	Yes	Yes	Yes
Observations	18,103	18,103	18,103	18,103	18,103	18,103	18,103	18,103	18,103

Notes: The dependent variable is the logarithm of the winning bid in Ethereum for an NFT auction (i) sold by seller (s) and won by buyer (a) at time (t). PQR stands for panel quantile regression, DR for distributional regression, and BC for bias-corrected DR. Standard errors are in parentheses. All models include a constant. Statistical significance levels are denoted as follows: *** indicates significance at the 1% level, ** at the 5% level, and * at the 10% level. Standard errors are enclosed in parentheses.

1.6 Conclusion

This research aims to shed light on the evolving dynamics of NFT markets, where traditional market structures are being reshaped by decentralized networks and digital connections. Our analysis shows that trading networks have direct effects on market prices, even in the absence of powerful market makers. Furthermore, a combination of a substantial follower count and a limited number of connections made by following others on the platform, can lead to significant price increases for popular sellers. Trading network effects for sellers are dominant for low valued NFTs, while the dynamics shift, and popularity gains importance for high-valued NFTs. On the other hand, buyers may see larger trading networks as validation for higher bids, but their involvement in the Foundation community does not appear to impact NFT prices.

Our research offers valuable insights that extend beyond the realm of NFTs for digital art. Our contribution to the empirical literature on networks and decision making, particularly through panel quantile and distributional regression analysis, can have broader applications in the study of online marketplaces. Our approach, which allows us to overcome estimation challenges and accounts for participant interdependencies, endogeneity, and potential estimation bias, can be applied to real estate sales, the market for financial securities, and e-commerce, to study factors that influence price formation across the distribution.

While our analysis allows us to control for Foundation connections we do not have detailed information on the structure of those connections. Future analysis could focus on an in-depth exploration of how the structure of the Foundation connections vis-a-vis the trading networks influences prices within the NFT market. This structure could also help us understand the relative influence on prices of individuals with followers versus those who follow others on the platform. Further research could also center on sentiment analysis, exploring the impact of positive or negative attitudes and emotions toward NFT assets thus adding an insight into additional forces that might shape market outcomes.

Chapter 2

Beyond Value: Investigating Reputation Effect on Resale Prices in NFT Auctions

The rise of digital art and the emergence of Non-Fungible Tokens (NFTs) have revolutionized the traditional art market, introducing new dynamics and challenges for market participants. As digital assets, NFTs provide a unique framework for understanding how networks and followers impact the resale price of art. Repeated auction sales have garnered significant attention due to their dynamic nature and potential for enhancing market efficiency. In this paper, we explore the intricate dynamics of repeated NFT auctions on the Foundation platform, with a particular focus on how buyer and seller reputation—reflected in the number of followers and information transmission, as indicated by Katz centrality of previous activity—affect resale prices.

The study of repeated auctions is a significant area within auction theory, examining how different auction designs and rules affect outcomes. Researchers analyze bidder behavior, auction formats, and market dynamics to understand and improve auction performance. Understanding the dynamics of repeated auction sales is crucial, as these mechanisms are pivotal in various markets, including online platforms like the Foundation. Participants in these decentralized markets continually adapt their strategies based on past outcomes, which influences market efficiency and dynamic pricing. These auctions are characterized by several key aspects:

- Learning and Adaptation: Participants, both buyers and sellers, refine their strategies based on historical outcomes. Buyers may adjust their bidding behavior to enhance their chances of winning at lower prices, while sellers select their reserve prices to maximize revenue.

- Reputation Effects: The reputation of both buyers and sellers plays a crucial role in repeated auctions. A well-regarded seller can attract higher bids, while a buyer with a history of winning auctions may influence the bidding behavior of others.

- Market Efficiency: Repeated auctions tend to lead to more efficient market outcomes as participants accumulate information about the value of items and the strategies of their competitors.

- Dynamic Pricing: Prices in repeated auctions can fluctuate based on demand, competition, and market conditions, allowing for dynamic price discovery and revealing the true market value of items.

Previous studies have highlighted the importance of reputation in online auctions. Bajari and Hortaçsu (2003) examined eBay coin auctions, revealing that seller reputation crucially influences auction revenues. Positive reputations increased revenues, while negative feedback could reduce revenues by up to 15%. Bidder experience, however, did not notably affect auction outcomes. Dellarocas (2005) explored reputation mechanisms in electronic markets, showing that simpler mechanisms, which publish only recent ratings, can achieve maximum efficiency by ensuring punishment for negative behavior. Bolton et al. (2008) found that competition enhances feedback systems' effectiveness in fostering trust and market efficiency. Ba and Pavlou (2002) demonstrated that proper feedback mechanisms foster trust and generate price premiums for reputable sellers. Lucking-Reiley et al. (2007) found that negative feedback significantly lowers auction prices for collectible coins, emphasizing the importance of maintaining a good reputation.

Khademorezaian et al. (2022) have studied the impact of networks and platform followers on NFT prices, specifically focusing on original sales within the Cryptoart market. Their research uncovers significant heterogeneous effects across the distribution of Cryptoart prices, providing valuable insights into how network connections and platform popularity influence market outcomes. Sellers with extensive trading networks and a significant number of followers are able to leverage the information and reputation built through these connections to achieve better sales outcomes for lower-priced NFTs. Their findings suggest that trading network effects for sellers are dominant for low valued NFTs while platform popularity gains importance for high valued NFTs. A combination of a substantial follower count and a limited number of connections made by following others on the platform can have a significant impact on the price of Cryptoart sold on the Foundation platform. On the buyer's side, the study reveals that there are no significant platform effects while network effects are more muted. Grover et al. (2022) in their survey paper on the evolution of social media influence underscore the limited exploration in the literature of topics such as information diffusion, and social media or platform influence in a market context. Their work emphasizes the need for more research to understand how social media and platform interactions shape market dynamics and outcomes. Oh et al. (2022b) assess investor performance in the NFT market with a particular emphasis on experience. While a broad network often suggests substantial experience, our research focuses on understanding the distinct effects of the sales network structure and platform reputation on resale prices.

In the context of art as an investment, constructing an accurate index of art prices has been challenging due to the heterogeneous nature of art objects and infrequent trading. The hedonic approach and the Repeat Sales Regression have been employed to compute the rate of return on paintings over time, each with its strengths and limitations (Ashenfelter and Graddy, 2006). NFTs offer a unique opportunity to assess price movements over time for digital art, which bears common value and does not depreciate in the traditional sense. This paper aims to analyze repeated auctions of NFTs on the Foundation platform, exploring the interplay between buyer and seller reputation and their implications for market dynamics. By shedding light on these dynamics, we contribute to a deeper understanding of the evolving landscape of digital asset markets and their parallels with traditional art markets. Through our analysis, we aim to provide insights into the factors driving the likelihood of resale and resale prices in the NFT market, offering valuable insights for participants and policymakers alike.

The remainder of the paper is organized as follows. Section 2 provides an overview of the Foundation platform and the data. Section 3 presents an empirical investigation of the impact of trading networks and platform connections on resale prices. Finally, Section 4 concludes with a summary of our findings.

2.1 Platform and Data Overview

Foundation, a platform dedicated to CryptoArt, launched in February 2021 with an invitation-based model that allows users to mint and sell NFTs directly. The platform supports various wallets and utilizes smart contracts to manage transactions. In particular, users mint new NFTs by uploading their Cryptoart, which is registered on the blockchain via a smart contract linked to their wallet. The process involves inputting metadata, and listing the NFT for sale. This process is decentralized without the use of intermediaries unlike sales in traditional auction markets mostly controlled by dealers. Ownership is recorded on the blockchain's distributed ledger, with sellers paying a percentage of subsequent sales as royalties to the original creator.

An NFT can be listed for sale with a "Buy Now" option or a reserve price for auction. The auction starts when a bid meets the reserve price and concludes 24 hours later. The highest bidder transfers the bid amount to the seller's wallet, and the NFT is transferred accordingly.

Foundation also functions as a social network, allowing users to follow profiles and build reputations through sales. The market experienced significant changes from rapid growth in early 2021 to maturity by mid-2022, aligning with Ethereum's price fluctuations. The number of auctions eventually stabilized post-cryptocurrency crash, with reduced volatility. Currently, the price of Ethereum has recovered most of its losses and is now at approximately 82 percent of its peak value, reinvigorating the level of activity on the platform.

We created a dataset of repeated sales from auctions on the Foundation platform, ranging from February 5, 2021, to December 5, 2022. We retrieved all auction data from the Ethereum blockchain via thegraph.com and identified the NFTs that were auctioned twice. We use the unique user IDs from the blockchain to retrieve additional information about the participants from the Foundation platform, including their number of followers, followings on the platform, and social media accounts. We collected auction information that includes the time of creation, the reservation price, history of any reservation price changes, and details about bidders and their bid amounts. We retrieve the Ethereum to US Dollar exchange rate from Etherscan.io, which tracks this information. After excluding auctions involving participants banned or suspended from the platform due to terms of service violations, the remaining count totals 1274 repeated sales. Table 1 provides summary statistics for the auctions used in our regression analysis during the period under consideration.[1] The average winning bid is of primary sales was 0.72 ETH, with a standard deviation of 1.35 ETH. The corresponding winning bid for NFT resales was 1.52 ETH, with a standard deviation of 3.54 ETH. On average, the duration between listing and final sale for primary sales was 30.4 hours while for secondary sales the listing to final sales was 58.13 hours. This duration offers a more realistic assessment of the time taken to successfully sell an NFT compared to the standard 24-hour auction duration. We classify participants into four groups based on their prior actions within the platform. A seller is defined as a participant who has successfully sold an NFT, while a collector is a participant who has won an auction. An artist refers to a creator who has minted an NFT, and a bidder is a participant who has placed bids at the auction, irrespective of whether they won the auction or not. There is a lot of overlap across participant groups. On average, there were 6.85 participants in each primary sale and 5.33 in the secondary sale. The latter group is dominated by the number of collectors. Sellers have a larger number of followers in primary sales and a smaller in secondary sales.

We use all the auctions that occurred during this period to construct a network of trades between sellers and buyers (Kranton and Minehart, 2001), where a node represents a user in the Foundation platform and an edge represents an auction weighted by the winning bid value in Ethereum. We measure the centrality of each node k at time t using:

[1] Due to the lack of availability of data for some of those measures created for the analysis we dropped 69 observations.

Figure 2.1: Heat Map of Average Percentage Change in Prices

$$kc_{k,t}(N_t) = \sum_l \sum_j \delta^l \mathbf{A}^l_{t,k,j}, \tag{2.1}$$

where N_t represents the network of sellers and buyers form the transactions in the last 30 days, but excluding those at t. $\mathbf{A}_t$ representing its corresponding adjacency matrix where $\mathbf{A}_{t,k,j} \neq 0$ indicates the presence of transactions between node k and j during the time frame before t. The index l denotes the length of walks emanating from node k and δ represents the discount factor. Following standard practice (Bloch et al., 2023), the discount factor is determined by establishing an upper bound based on the maximum eigenvalue of matrix $\mathbf{A}_t$.

Figure 2.1 presents a heat map showing the average percentage change in prices across quartiles, based on the number of followers and accounts followed by original sellers/creators, secondary sellers, and buyers. The data suggests that price changes tend to be higher for creators and secondary buyers with many followers but who follow few others. In contrast, no clear pattern emerges for secondary sellers. To better understand the impact of sales networks and follower counts on prices, our regression analysis will control for NFT characteristics, auction details, and bidder profiles.

Finally, for each NFT, we obtained the creator's unique blockchain identifier, mint date,

Figure 2.2: Log-transformed Auction Prices

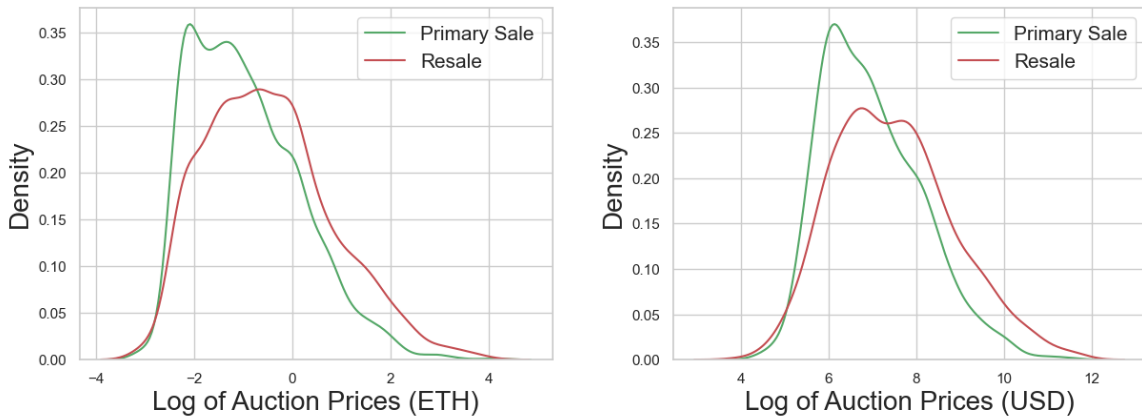

Note: The plot on the left displays the density plot of the logarithm of the winning bids in Ethereum. The plot on the right uses the exchange rate at the time of the auction to convert these values into US Dollars.

and IPFS path, allowing us to locate the NFT's metadata. Using these addresses, we retrieved metadata from ipfs.tech, which includes the NFT's name, description, and link to the stored file. We used this link to extract both the file name and its extension, enabling us to identify the specific file type. We categorized the files into three groups: static images (.jpg, .png, .svg), animated files (.gif, .mov, .mp4), and 3D images (.glb, .gltf). Creators often add descriptions, averaging around 212 characters. There were no 3D images resold in this market with 59 % of the images that sold twice being still. Summary statistics for the NFTs are listed in Table 1.

Figure 2.2 presents the density of winning bids in both Ethereum and USD, indicating that resale prices tend to be higher overall with the main differentiation happening beyond the lower valued NFTs.

Figure 2.3 presents additional information on the percentage price change between the primary and secondary sales. Based on this data, only 25% percent of Cryptoart experienced

Table 2.1: Descriptive Statistics

	Primary Sale					Secondary				
Variable	Mean	Deviation Standard	Min	Max	Number of Observations	Mean	Deviation Standard	Min	Max	Number of Observations
A. Summary of Auctions										
Winning Bid Amount	0.72	1.35	0.05	19.80	1,205	1.52	3.54	0.05	50.00	1,205
Listing-to-Sale duration (Hours)	14.45	30.40	1.00	387.42	1,205	58.13	78.80	0.96	529.34	1,205
Reservation Price Change	0.23	0.42	0.00	1.00	1,205	0.37	0.48	0.00	1.00	1,205
B. Participants Type in Auctions										
No. of Bidder Never Won	0.18	0.67	0.00	10.00	1,205	0.08	0.53	0.00	9.00	1,205
No. of Artist and Seller	0.77	1.02	0.00	7.00	1,205	0.02	0.15	0.00	2.00	1,205
No. of Artist and Collector	2.29	2.32	0.00	19.00	1,205	1.15	1.69	0.00	12.00	1,205
No. of Collector	2.91	2.67	0.00	18.00	1,205	4.08	2.40	0.00	20.00	1,205
C. Network and Social Media										
Katz Centrality of Seller	0.02	0.08	0.00	1.00	1,205	0.01	0.06	0.00	1.00	1,205
Katz Centrality of Buyer	0.02	0.08	0.00	1.00	1,114	0.06	0.17	0.00	1.00	1,205
No. of Followers of Seller	1322.64	1620.82	3.00	13000.00	1,205	1233.32	1661.24	12.00	12900.00	1,205
No. of Seller Following	402.97	2932.01	0.00	93700.00	1,205	344.32	1892.92	0.00	41900.00	1,205
No. of Followers of Buyer	1197.40	1630.78	6.00	9611.00	1,205	1810.83	2564.68	4.00	12600.00	1,205
No. of Buyer Following	290.27	978.05	0.00	16100.00	1,205	210.73	427.25	0.00	3581.00	1,205
Seller has Twitter	0.96	0.19	0.00	1.00	1,205	0.77	0.42	0.00	1.00	1,205
Seller has Instagram	0.78	0.42	0.00	1.00	1,205	0.44	0.50	0.00	1.00	1,205
Buyer has Twitter	0.73	0.44	0.00	1.00	1,205	0.62	0.49	0.00	1.00	1,205
Buyer has Instagram	0.39	0.49	0.00	1.00	1,205	0.24	0.43	0.00	1.00	1,205
D. NFT characteristics										
Length of NFT's Description	212.49	202.77	0.00	1000.00	1,205					
Still Image	0.59	0.49	0.00	1.00	1,205					
Animated	0.41	0.49	0.00	1.00	1,205					
3D Format	0.00	0.03	0.00	1.00	1,205					

Notes: The computation of Katz centrality follows (2.1). The description of participant types in Panel B is explained in section 2.1.

a price decline in secondary sales. The distribution is skewed to the right with a few sales (49 sales in terms of USD and 29 in ETH) achieving an appreciation of more than 10%. As the left bottom panel of the figure suggests, most of the NFTs that resold at the beginning of the time window, during the periods of initial market surge and eventual stabilization, experienced more significant price increases. Those resold many months after their initial sale experienced smaller increases in price, and sometimes decreases, with greater fluctuations in the percentage change for those sold 10 months or more after the initial sale. The bottom right panel confirms that resale returns were higher in the earlier part of our time window.

Finally, Figure 2.4 shows that primary and secondary sales volume decreased in the latter part of the period coinciding with the crush of the cryptocurrency market. The figure captures the daily number of transactions for all NFTs that were resold in the entire period peaking around the time when Ethereum value was at its highest.

2.2 Empirical Analysis

In this section, we will consider how the relative price of an NFT is affected by trading networks and buyer and seller popularity. We will also examine the factors that affect the probability of a resale.

2.2.1 Resale Price

We first estimate the change in relative price when an NFT is resold as a fuction of auction, NFT and bidder characteristics including network variables capturing popularity and trading

Figure 2.3: Percentage Change in Price between Primary and Secondary

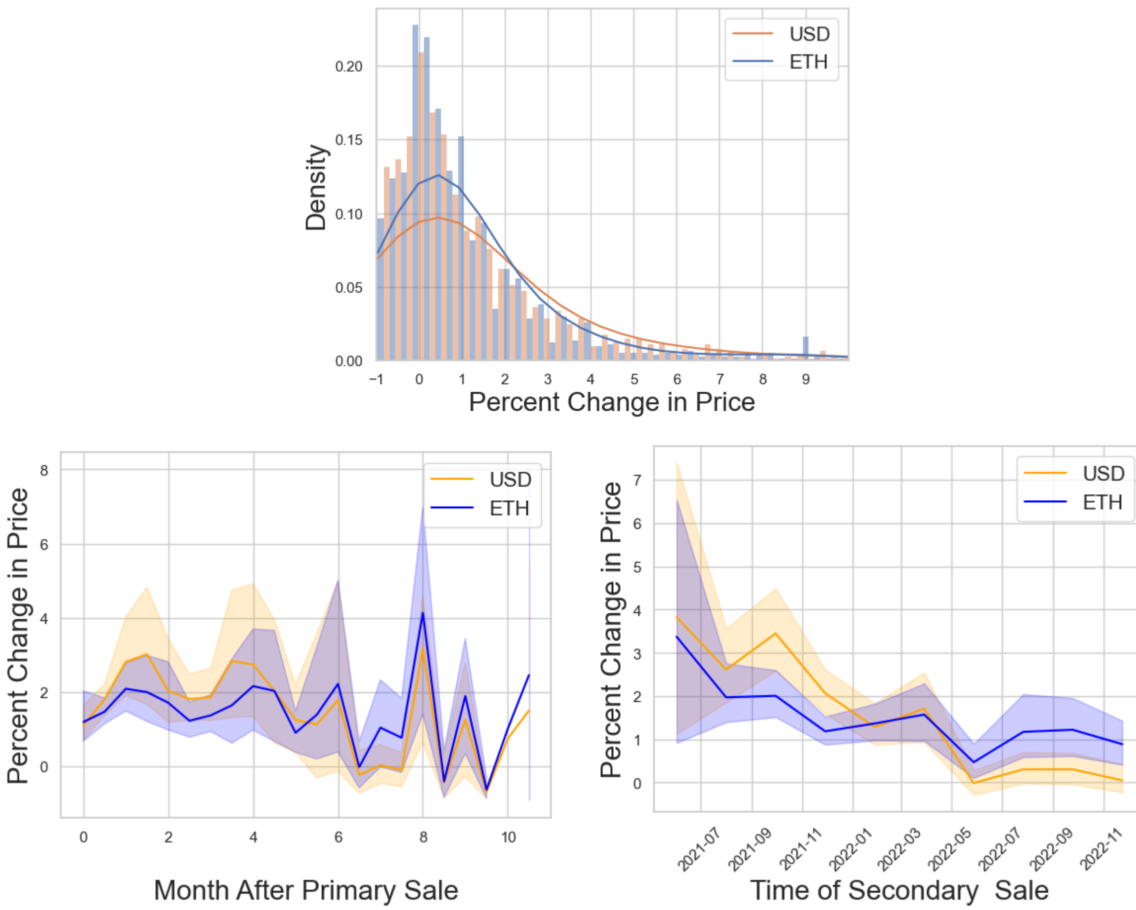

Note: The exchange rate at the time of sale is used to calculate the value in USD. In the top figure, there are some observations spread above 10 percent, with very low density (49 in USD and 29 in ETH), that are not shown in the figure for better visualization. On the left, the figure shows the density of change in resale price. The plot on the right charts this percentage change over the period between the two sales. The lines denote the mean, while the shaded areas represent the 95th percentile.

Figure 2.4: Primary and Secondary Sales over Time

Note: The lines are the average number of actions for each month and the shaded areas are the 95th percentiles.

experience. We consider the following semiparametric equation:

$$\log(\frac{y_{isrt_2}}{y_{iast_1}}) = \boldsymbol{N}'_{isrt_2}\boldsymbol{\delta}_1 + \boldsymbol{F}'_{iasrt_2}\boldsymbol{\delta}_2 + \boldsymbol{W}'_{isrt_2}\boldsymbol{\theta} + f_d(D_{it_2}) + f_e(E_{t_2}) + \mu_{t_2} + u_{iasrt_2}, \qquad (2.2)$$

where y_{isrt_2} denotes the winning bid of an NFT i, bought by buyer r, and sold by seller s at time t_2 and y_{iast_1} denotes the winning bid received by the creator a at time t_1 paid by buyer s. The vector $\boldsymbol{N}_{isrt_2}$ denotes network variables at the time of resale and $\boldsymbol{F}_{iasrt_2}$ includes the number of accounts following creators, buyers, and sellers on the Foundation platform, and the number of accounts the creator, buyer or the seller follows. The vectors $\boldsymbol{W}_{isrt_2} = (\boldsymbol{S}'_{isrt_2}, \boldsymbol{B}'_{it_2}, \boldsymbol{X}'_i)'$ include various controls. $\boldsymbol{S}_{isrt_2}$ contains indicators for social media presence (i.e, the buyer has a Twitter or Instagram account connected to the Foundation platform), $\boldsymbol{B}_{it_2}$ are auction-related controls, including bidder type and an indicator denoting changes in the reservation price, and the time between the primary and secondary sale, $\boldsymbol{X}_i$ are NFT related controls including the type of NFTs auctioned off and the length of their description. μ_{t_2} are time dummies and u_{iasrt_2} is an error term.

The model also includes two unknown functions in terms of the listing-to-sale duration of the auction D_{it_2} and the exchange rate E_{t_2}. We estimate the functions f_e and f_d using cubic B-spline functions with five knots. A detailed description of all the variables used in our analysis is provided in Table A2.1 in the appendix.

The first column of Table 2.2 provide the mean level regression results and the following columns present the estimated coefficients at various quantiles. The number of followers of the primary seller capturing the popularity of the creator, has a positive effect on the rate of change of prices. This effect is significant for low quartiles and at the median. In other words, the seller's popularity drives small changes in the price but is not having an effect in NFTs whose prices increased substantially. The number of accounts that the creator follows does not seem to make a discernible difference. The popularity of the secondary seller, which is also the buyer in the primary sale does not have a statistically significant impact on the price ratio which suggests that the buyers in the secondary market rely more on the popularity of the first seller and creator of the NFT to determine its value than on the seller who resales. The number of accounts following the secondary buyer have a positive impact and the number of accounts followed have a negative impact. These effects increase across quantiles, indicating that more popular buyers in the secondary market generate relatively higher prices.

Table 2.2: Estimation Results of Price Ratio

	OLS	Q0.1	Q0.25	Q0.5	Q0.75	Q0.9
Number of Followers Primary Seller	0.093***	0.073**	0.082***	0.097***	0.047	0.049
	(0.028)	(0.036)	(0.031)	(0.029)	(0.037)	(0.056)
Number of Following Primary Seller	−0.025	−0.020	−0.018	−0.020	0.003	−0.006
	(0.018)	(0.024)	(0.020)	(0.020)	(0.024)	(0.036)
Number of Followers Secondary Seller	−0.019	−0.033	−0.016	−0.017	0.018	0.082*
	(0.026)	(0.036)	(0.029)	(0.028)	(0.034)	(0.048)
Number of Following Secondary Seller	0.009	−0.004	0.008	0.004	−0.017	−0.029
	(0.018)	(0.026)	(0.018)	(0.018)	(0.025)	(0.035)
Number of Followers Secondary Buyer	0.208***	0.134***	0.103***	0.141***	0.230***	0.274***
	(0.023)	(0.032)	(0.025)	(0.027)	(0.033)	(0.042)
Number of Following Secondary Buyer	−0.161***	−0.100***	−0.077***	−0.127***	−0.197***	−0.234***
	(0.020)	(0.025)	(0.021)	(0.024)	(0.027)	(0.034)
Centrality Secondary Seller	0.205	−0.001	0.468	0.156	0.154	−0.304
	(0.384)	(0.509)	(0.384)	(0.372)	(0.367)	(0.348)
Centrality Secondary Buyer	0.572***	0.454***	0.337**	0.436**	0.711**	0.740**
	(0.160)	(0.165)	(0.143)	(0.178)	(0.287)	(0.372)
Months from Primary Sale	−0.041***	−0.130***	−0.090***	−0.030**	−0.015	0.015
	(0.012)	(0.022)	(0.022)	(0.014)	(0.018)	(0.020)
Auctions Controls	Yes	Yes	Yes	Yes	Yes	Yes
NFT Controls	Yes	Yes	Yes	Yes	Yes	Yes
Semiparametric Functions	Yes	Yes	Yes	Yes	Yes	Yes
Month and Year Dummies	Yes	Yes	Yes	Yes	Yes	Yes
Social Media Variables	Yes	Yes	Yes	Yes	Yes	Yes
Observations	1,205	1205	1,205	1,205	1,205	1,205

Notes: The dependent variable is the logarithm of the ratio of the winning bid in the primary sale to the secondary in Ethereum for an NFT. Number of followers and following are logged. All models include a constant. Statistical significance levels are denoted as follows: *** indicates significance at the 1% level, ** at the 5% level, and * at the 10% level. Standard errors are enclosed in parentheses.

Table 2.3: Secondary Price Estimation Results

	OLS	Q0.1	Q0.25	Q0.5	Q0.75	Q0.9
Primary Sale Price	0.638***	0.629***	0.712***	0.747***	0.691***	0.660***
	(0.031)	(0.047)	(0.038)	(0.036)	(0.045)	(0.061)
Number of Followers Primary Seller	0.196***	0.197***	0.164***	0.132***	0.147***	0.173***
	(0.028)	(0.041)	(0.032)	(0.031)	(0.040)	(0.060)
Number of Following Primary Seller	−0.077***	−0.080***	−0.070***	−0.051**	−0.042	−0.039
	(0.018)	(0.025)	(0.020)	(0.021)	(0.026)	(0.036)
Number of Followers Secondary Seller	0.041	0.010	0.004	0.033	0.047	0.049
	(0.025)	(0.032)	(0.028)	(0.028)	(0.032)	(0.045)
Number of Following Secondary Seller	−0.022	−0.004	−0.018	−0.013	−0.023	−0.005
	(0.018)	(0.024)	(0.019)	(0.019)	(0.024)	(0.030)
Number of Followers Secondary Buyer	0.249***	0.159***	0.164***	0.208***	0.245***	0.364***
	(0.022)	(0.031)	(0.026)	(0.028)	(0.032)	(0.045)
Number of Following Secondary Buyer	−0.182***	−0.102***	−0.109***	−0.170***	−0.202***	−0.279***
	(0.019)	(0.025)	(0.022)	(0.025)	(0.026)	(0.034)
Centrality Secondary Seller	0.300	−0.309	0.612*	0.279	0.526	0.297
	(0.363)	(0.508)	(0.327)	(0.440)	(0.375)	(0.421)
Centrality Secondary Buyer	0.552***	0.285*	0.254*	0.317*	0.582**	0.581
	(0.151)	(0.172)	(0.138)	(0.169)	(0.237)	(0.373)
Months from Primary Sale	−0.020*	−0.092***	−0.057***	−0.026*	0.007	0.021
	(0.011)	(0.024)	(0.018)	(0.014)	(0.019)	(0.019)
Auctions Controls	Yes	Yes	Yes	Yes	Yes	Yes
NFT Controls	Yes	Yes	Yes	Yes	Yes	Yes
Semiparametric Functions	Yes	Yes	Yes	Yes	Yes	Yes
Month and Year Dummies	Yes	Yes	Yes	Yes	Yes	Yes
Social Media Variables	Yes	Yes	Yes	Yes	Yes	Yes
Observations	1,205	1205	1,205	1,205	1,205	1,205

Notes: The dependent variable is the logarithm of the winning bid in Ethereum from the secondary sale. Number of followers and following are logged. All models include a constant. Statistical significance levels are denoted as follows: *** indicates significance at the 1% level, ** at the 5% level, and * at the 10% level. Standard errors are enclosed in parentheses.

Here, the resale seller as the middleman between the creator and the second buyer does not have substantial effect on relative prices. Buyers with extensive networks are more inclined to bid up prices in the secondary market and that is more significant at the upper quartiles. Lastly, the number of months that elapsed since the primary sale, negatively impacts the price. In this analysis, the creator's popularity and the popularity and network of the buyer in the secondary sale are the most critical factors affecting change in relative prices. The secondary seller's experiences has a no statistically significant effect.

Table 2.3 presents a logarithmic model of the resale price as a function of the logarithm of primary sale price and other NFT, auction, bidder characteristics and time controls. Here we don't only see the relative price movements but we can see if the characteristics of bidders such as popularity and experience have a differential effect on prices across the distribution, conditional on the price levels achieved in the primary market. As in table 2, our results reveal that the popularity of the creator and the buyer in the resale market were critical in boosting the sales price. While the seller's popularity is affecting prices uniformly across quartiles, the popularity and experience of the secondary buyer has a larger effect at higher quartiles.

2.2.2 Likelihood of Resale

In this section, we examine the likelihood of resale as a function of the network ($\boldsymbol{N}_{iast}$) and Foundation variables ($\boldsymbol{F}_{iast}$) to investigate the effect of popularity and network connections in the primary sale on the probability of resale. We estimate the following Probit model:

$$\begin{aligned}\Pr(R_{ias} = 1 | y_{iast_1}, \boldsymbol{N}_{iast_1}, \boldsymbol{F}_{iast_1}, \boldsymbol{W}_{iast_1}, D_{it_1}, E_{t_1}, \mu_{t_1})\\ = \Phi(y_{iast_1} + \boldsymbol{N}'_{iast_1}\boldsymbol{\delta}_1 + \boldsymbol{F}'_{iast_1}\boldsymbol{\delta}_2 + \boldsymbol{W}'_{iast_1}\boldsymbol{\theta} + f_d(D_{it_1}) + f_e(E_{t_1}) + \mu_{t_1}),\end{aligned} \tag{2.3}$$

where $(R_{ias} = 1)$ denotes an NFT that will be resold in the future, and it equals one if we observe another auction for this NFT in our sample. We use the primary sales data. We are interested in the probability of resale based on primary sale value (y_{iast_1}), sales network $(\boldsymbol{N}_{iast})$ and Foundation followers $(\boldsymbol{F}_{iast})$. Variable $\boldsymbol{W}_{isrt_1} = (\boldsymbol{S}'_{iast_1}, \boldsymbol{B}'_{it_1}, \boldsymbol{X}'_i)'$ contains the NFT characteristics such as file type, length of description and types of participants in the auction.

Table 2.4 presents the estimation results of Equation 2.3. Column (1) presents the results using all auctions. Because some NFTs may not have had sufficient time to be resold, we use different subsamples of the auctions as control groups. Column (2) presents the results using NFTs that their original sales is before 2022. This is based on Figure 2.4, which shows that the majority of primary sales for resold items occurred by that time. In the next columns, we use propensity score matching to select a subsample of auctions without resale. The concern is that the treated and control groups (the NFTs that were resold and those that didn't during our sample period) may share different characteristics along a number of dimensions including the type of art, the timing of sale and the ETH exchange rate after the item was first sold. In this effort, we use subsamples of the control group that best mimic the treatment group in these dimensions.

We used nearest neighbor matching to select a control group. This process involves calculating the distance between observations. We used logistic, random forests, and Mahalanobis distances, which are commonly used in matching methods (Abadie and Imbens, 2016; Athey and Imbens, 2019), and picked the closest observation without replacement. The logistic distance is the predicted values of a GLM model with a binomial link, random forests uses the predicted values of fitted forest, and the Mahalanobis distance is defined as $d_{i,j} = \sqrt{(x_i - x_j)\Sigma^{-1}(x_i - x_j)'}$, where Σ is the pooled within-group covariance matrix of covariates computed by the treatment group-mean. Column (3) uses random forests and finds the 5 nearest neighbors, and Column (4) uses only the nearest neighbor. Column (5) uses logistic distance as scores and column (6) uses Mahalanobis distance. As mentioned above, we used auction and NFT-specific controls, time, and exchange rates for matching. The matching is performed across all auctions without resale. We then run our regression on network variables. Table A2.2 compares these matching processes by examining the means of matched variables. The matched variable means are closer to those of auctions with resales, creating a more effective control group.

The results suggest that the likelihood of resale is lower when prices in the original sale are higher. Additionally, the number of followers of a seller and creator has a positive impact on resale likelihood, while the number of accounts the seller is following has a negative impact. The number of followers a buyer has impacts negatively the likelihood of resale, whereas the number of accounts the buyer is following increases the likelihood. Popular buyers typically drive prices up in the original sale creating less opportunity for a bargain buy in a secondary market. The centrality of the seller does not impact the likelihood of resale when the sample is reduced to create a balance with respect to auction and NFT-specific controls, time, and exchange rates, but the centrality of the buyer decreases the likelihood. This indicates that more experienced traders are less likely to sell the NFTs they acquire.

2.3 Conclusion

In conclusion, our analysis reveals that the popularity of both primary sellers (creators) and secondary buyers significantly influences NFT price dynamics and resale likelihood. The primary seller's popularity drives modest price increases, particularly at lower price levels,

Table 2.4: Likelihood of Resale

	(1)	(2)	(3)	(4)	(5)	(6)
Winning Bid	−0.069***	−0.075***	−0.086***	−0.133***	−0.140***	−0.055*
	(0.016)	(0.018)	(0.021)	(0.030)	(0.029)	(0.030)
Number of Followers Seller	0.272***	0.292***	0.385***	0.447***	0.344***	0.308***
	(0.014)	(0.017)	(0.021)	(0.031)	(0.030)	(0.029)
Number of Following Seller	−0.062***	−0.072***	−0.089***	−0.108***	−0.091***	−0.086***
	(0.009)	(0.010)	(0.013)	(0.019)	(0.019)	(0.019)
Number of Followers Buyer	−0.149***	−0.147***	−0.187***	−0.220***	−0.201***	−0.205***
	(0.013)	(0.015)	(0.018)	(0.027)	(0.026)	(0.026)
Number of Following Buyer	0.108***	0.103***	0.129***	0.141***	0.116***	0.133***
	(0.011)	(0.012)	(0.015)	(0.021)	(0.021)	(0.020)
Centrality Seller	0.326*	0.346*	0.294	−0.332	0.545	0.032
	(0.167)	(0.203)	(0.255)	(0.326)	(0.407)	(0.360)
Centrality Buyer	−0.791***	−0.894***	−0.952***	−1.032***	−1.245***	−0.875***
	(0.142)	(0.174)	(0.194)	(0.253)	(0.243)	(0.261)
Auctions Controls	Yes	Yes	Yes	Yes	Yes	Yes
NFT Controls	Yes	Yes	Yes	Yes	Yes	Yes
Month and Year Dummies	Yes	Yes	Yes	Yes	Yes	Yes
Social Media Variables	Yes	Yes	Yes	Yes	Yes	Yes
Observations	82,091	44,585	7,710	2,570	2,570	2,570

Notes: The dependent variable is resale ($R \in \{0,1\}$). Number of followers and following are logged. All models include a constant. Statistical significance levels are denoted as follows: *** indicates significance at the 1% level, ** at the 5% level, and * at the 10% level. Standard errors are enclosed in parentheses.

while the secondary buyer's popularity tends to boost prices more significantly in higher quantiles. Interestingly, the centrality of secondary sellers has no statistically significant effect on prices. On the one hand, when considering relative prices, if the popularity and information acquired by a buyer in the primary market (seller in resale market) do not change much between sales the relative price is not expected to change a lot. On the other hand, if you consider the logarithm of prices, modeling the NFT auction as a common value auction as in Khademorezaian et al. (2022), we expect the information coming from the buyer in the primary sale (seller in the secondary sale) to affect the price as it adds valuable information about the perception of the value at the auction, Nevertheless, the price in the primary auction already incorporates the information coming from bidder participation at this auction. As long as this participant does not gain new insights, the auction price in the resale market will not be affected substantially. Buyers with extensive networks, however, bid up prices in resale and more so at the upper quartiles. The likelihood of resale is inversely related to the original sale price and positively influenced by the seller's popularity, yet negatively impacted by the buyer's popularity. These findings suggest that highly networked and experienced market participants are more strategic and selective in their trading, underscoring the nuanced role of social dynamics and market experience in shaping NFT market behavior.

Chapter 3

Route networks in the US Airline Industry

The route network of airlines is complex, resulting from multiple entry and exit decisions over the years. An airline's decision to enter or exit a route has a broader impact than just on the origin and destination. Most airlines use routes not only for point-to-point passenger transport but also as connections to facilitate serving other markets. In other words, the decision to serve a route will have spillover effects on other routes that the airline serves. This impact could arise from serving new origins and destinations or from the creation of shorter or alternative connections between two endpoints using connecting flights.

Most markets in the US are operated by multiple airlines, making route entry more complicated. Airlines compete in these markets, and when a competitor serves a market, it can intensify competition in other markets due to the spillover effects created in the competitor's route network.

In order to gain insight to the spillover effects resulting from the airlines route network, we use network theory to disentangle these effects. our contribution to the route entry literature is considering the spillover effect of entering a route for on airlines own route network and the competition from the other airlines when the airline faces competition not only from the specific route but also from the spillover of other routes served by the competitors.

The existing literature on route entry decisions defines markets or products differently. Some studies treat routes as simply origin and destination pairs without distinguishing between direct and connecting flights (Ciliberto and Williams, 2014; Berry, 1990, 1992). Others consider direct and connecting flights as differentiated products (Goolsbee and Syverson, 2008; Dunn, 2008). In recent literature, routes are often considered as a network of nodes (airports) and edges (flights), with routes defined between two airports (Aguirregabiria and Ho, 2010, 2012; Ciliberto et al., 2019; Brueckner, 2004; Gaggero and Piazza, 2021; Fu et al., 2019). This network approach allows for analyzing the potential effects of route choices on other routes, but edges alone do not encompass all markets. In network terminology, our market definition is a path in the network, accommodating both connecting and direct flights between an origin and destination. [1]

The literature on route entry, which accounts for the spillover effect in entry decisions, shows that airlines base their entry choices on the entire route network. This approach may lead airlines to operate on routes with negative profits if it ultimately increases their overall profit. Aguirregabiria and Ho (2010, 2012) demonstrate that in a hub-and-spoke network, an airline's profit function is supermodular regarding its own entry decisions for different city pairs. Orzach and Dix (2021) show that traditional estimates of consumer surplus effects from airline entry events and mergers tend to underestimate the impact due to the positive pass-through between direct and connecting fares. Fu et al. (2019) identify airport presence

[1] A walk is a general way to move from one node to another, whereas a path is a specific type of walk that does not visit any node more than once. In the context of the U.S. route network, this is equivalent to going from airport A to C with a connection at B.

and substitutability between airport-pair markets as sources of network effects.

Our work is most similar to Orzach and Dix (2021), which looks at airlines as multi-product firms. They show that a demand shock to one route can impact other routes with related costs. They also found that many indirect flights saw fare changes after mergers, even when the number of competitors on those indirect routes didn't change.

When considering the spillover effects of route entry on a route network, competition on a specific route can increase due to competitors entering other routes. Extensive research has examined the impact of competition on pricing by analyzing the presence of competitors on a route (Ciliberto and Tamer, 2009; Berry and Jia, 2010). Some studies distinguish between low-cost carriers (LCCs) and regional airlines (Gerardi and Shapiro, 2009), or direct and non-stop flights (Dunn, 2008). They often use measures such as the number of carriers on a route, the Hirschman-Herfindahl Index (HHI), the presence of LCCs, and the share of total traffic by each airline at each airport to measure the competitive effects (Goolsbee and Syverson, 2008; Dai et al., 2014; Mazzeo, 2003).

Several studies have modeled the interdependencies across markets in entry decisions. For example, Benkard et al. (2018) modeled the entry decisions of carriers jointly across route segments. Their model considers the features of each carrier's own route network as well as the networks of other airlines to capture the medium and long-term dynamic effects of horizontal mergers. Zhang and Wang (2016) examined the impact of low-cost airlines from the perspective of airports and time by a dynamic spillover effect function.

In the literature on airline network competition that endogenizes the route network, our work is similar to Yuan (2020). However, our study differs as we focus on finding the magnitude of competition at the route level, considering that the competition could spillover from other routes in the competitor network.

This paper aims to analyze airline route network choices by examining the spillover effects between routes. By considering markets that serve as connections and the impact of operating on one market on others, both for the airline and its competitors, this study contributes to a better understanding of airline route network decisions. Our findings suggest that airlines are more inclined to operate on routes that serve as connections and have higher spillover effects (influencing more markets as connections). Furthermore, airlines are more likely to enter routes with greater competition.

3.1 Data and Variables

We use the Origin and Destination Survey (DB1B), a 10% sample of airline tickets from reporting carriers collected by the Office of Airline Information of the Bureau of Transportation Statistics, to identify markets from the first quarter of 2017 to the fourth quarter of 2023. We restrict our sample to itineraries where both the origin and destination are within the United States, excluding airports in U.S. territories. We define a market as a directional pair of origin and destination. Using the DB1B-ticket data, we identify and exclude ground transportation or interlining itineraries. Additionally, we omit multi-way tickets, which are defined as those with more than two destinations.

The DB1B-coupon data includes the sequence of coupons for each market within an itinerary, allowing us to reconstruct the travel path for each market. For example, in the first quarter of 2022, American Airlines served the market from Will Rogers World Airport (OKC) to LaGuardia Airport (LGA) directly, or with connections through Dallas/Fort Worth International (DFW), Charlotte Douglas International (CLT), Chicago O'Hare International (ORD), and Ronald Reagan Washington National (DCA).

We use the T-100 Domestic Market dataset from the Bureau of Transportation Statistics to identify seasonal flights. The T-100 dataset reports all flights within a month, including information on air carriers, origins, destinations, and service classes for enplaned passengers. We retain markets with more than 10 enplaned passengers per month and that have scheduled flights operated by any airline for at least six consecutive months.

After eliminating seasonal flights from the DB1B data, we are left with 5,342 routes among 287 airports. Similar to Ciliberto and Tamer (2009), we exclude markets that are not served by any airline. Additionally, we exclude markets that could be served by each airline, but where neither the origin nor the destination is served by that airline. Table 3.1 presents the list of airlines along with the average number of market they operate from the beginning of 2017 to the end of 2023. We used the Master Coordinate from the aviation support tables to identify the geolocation of each airport and used the airport locations to retrieve weather and demographic information.

Our sample includes 10 ticketing carriers: American Airlines (AA), Alaska Airlines (AS), JetBlue (B6), Delta Air Lines (DL), Frontier Airlines (F9), Allegiant Air (G4), Spirit Airlines (NK), Sun Country Airlines (SY), United Airlines (UA), and Southwest Airlines (WN). [2]

We utilize the US Census Bureau to determine the Metropolitan/Micropolitan Statistical Areas for each airport. For airports not located within any Metropolitan or Micropolitan area, we use county-level data. Out of 287 airports, 237 were situated in Metropolitan areas, 41 in Micropolitan areas, and 9 were not located within any designated statistical area.

We obtain the monthly unemployment rate for each airport from the Local Area Unemployment Statistics (LAUS) program of the Bureau of Labor Statistics (BLS) within the U.S. Department of Labor. This program provides monthly estimates of total employment and

[2] We exclude Virgin America (VX), which began reporting jointly with Alaska Airlines (AS) from April 2018 following their 2016 merger announcement.

Table 3.1: Number of Routes

Carrier	Mean	Standard Deviation	Min	Max	Number of Quarters
AA	5215.54	16.40	5158	5239	28
AS	3938.54	416.05	2610	4546	28
B6	3290.54	649.68	967	4197	28
DL	5162.71	79.15	4796	5212	28
F9	3916.39	602.70	1856	4585	28
G4	3477.64	365.36	2714	4015	28
NK	3322.57	469.27	1608	4017	28
SY	591.50	353.21	178	1493	28
UA	5138.39	91.54	4699	5204	28
WN	4857.29	159.59	4648	5049	28

Note: Number of observed and potential origin-destination pairs for each carrier from the first quarter of 2017 to the last quarter of 2023.

Table 3.2: Descriptive Statistics

Variable	Mean	Standard Deviation	Min	Max	Number of Observations
A. Demographics					
Population	7.458	0.772	4.672	9.701	1,042,959
Per Capita Income	4.089	0.190	3.405	5.322	1,042,959
Wage	9.356	1.533	3.623	12.418	1,042,959
Unemployment Rate	4.376	2.154	1.833	29.433	1,042,959
B. Weather					
No. Freezing Days	2.842	5.734	0.000	64.000	1,042,959
Snow (Millimeters)	98.154	187.404	0.000	2320.500	1,042,959
Precipitation (Millimeters)	233.118	166.553	0.000	1185.250	1,042,959
Average Temperature (C)	14.243	7.330	-13.940	30.224	1,042,959
Maximum Temperature (C)	19.539	7.625	-9.860	38.353	1,042,959
Minimum Temperature (C)	8.946	7.149	-18.020	25.649	1,042,959

Notes: Population is the logarithm of the geometric mean of the populations (in thousands) of the origin and destination. Per capita income and wages (in thousands of US dollars) are in logarithmic form and averaged between the origin and destination. The unemployment rate and all weather variables are averages of the origin and destination values.

unemployment rates. We then aggregate these monthly unemployment rates into quarterly data. We acquire quarterly wage data from another survey conducted by BLS called the Quarterly Census of Employment and Wages (QCEW) program. This program publishes a quarterly count of employment and wages reported by employers, covering over 95 percent of U.S. jobs available at the county level. Other demographic factors such as population, per capita personal income, and personal income are sourced from the Bureau of Economic Analysis. These values are reported annually. We measure market size using the logarithm of the geometric mean of the populations at the origin and destination. For per capita income, wages, and the unemployment rate, we use the average of the origin and destination values. A summary of these measures is provided in Panel A of Table 3.2.

We obtained weather data from the Global Summary of the Month (GSOM) published by NOAA National Centers for Environmental Information. This dataset provides monthly meteorological elements dating back to 1763, with weekly updates. We began by identifying the nearest weather station to each airport and retrieved metrics such as average, minimum, and maximum monthly temperature, total monthly precipitation, total monthly snowfall, and the number of days with maximum temperature below 32 degrees Fahrenheit (0 degrees Celsius), and aggregated this information into quarterly data for each airport. We use the average values from the origin and destination for each market. A summary of these measures is provided in Panel B of Table 3.2.

3.2 Model

There are N airlines indexed by i that decide whether to enter into the market $m_i = 1, ..., M_i$ at time $t = 1, ..., T$ and $M_i \subset M$ is a subset of all markets available for airlines. For simplicity, we omit the route index in the notation. If firm i enters market m at quarter t, we assume that the profit of that route is positive and denote this event as $\pi_{imt} > 0$. Airlines observe the route networks of their competitors from that last quarter and all airlines simultaneously decide on their route networks for the current quarter, taking into account market characteristics, their network and past networks of their competitors. Firm's i profit is:

$$\begin{aligned} \pi_{imt} &= \beta' \boldsymbol{S}_{imt} + \delta' R_{i,t} + \eta E(a|\boldsymbol{S}_{mt}, R_{-i,t}) + \epsilon_{imt} \\ &= \gamma \boldsymbol{X}_{mt} + \boldsymbol{w}_{mt} + \psi_i + \zeta_t + \theta_m + \alpha \Delta c_{imt} D_{imt} + HS_{imt} + \hat{H}_{-imt} + \epsilon_{imt}, \end{aligned} \tag{3.1}$$

The vector $\boldsymbol{S}_{imt}$ contains variables that influence airline i's choice of market m in quarter t, including carrier unobserved heterogeneity that we control by the carrier fixed effect ψ_i. The vector $\boldsymbol{S}_{mt}$ is a subset of $\boldsymbol{S}_{imt}$ and includes covariates that affect the decisions of all airlines. It includes vector $\boldsymbol{X}_{mt}$, which represents route characteristics, and vector $\boldsymbol{w}_{mt}$, which contains weather measures. Additionally, we control for the unobserved heterogeneity of the route and time using ζ_t and θ_m.

$R_{i,t}$ represents the route network of airline i at quarter t. It includes the change in centrality from the previous period Δc_{imt}, the indicator D_{imt} which signifies whether market m was used as a connection for other markets in the past period, and HS_{imt}, which captures the impact of this market on other markets. We use $R_{-i,t}$ to denote the route network of all competitors.

The term $E(a|\boldsymbol{S}_{mt}, R_{-i,t})$ captures the expected competition on the market, given the route network of competitors and the market characteristics observed by all airlines. $\hat{H}_{-imt}$ denote the estimate expected competition from the competitors. Finally, ϵ_{imt} is the error term, following an extreme value distribution.

3.3 Route Network

We create a network of routes for each airline in each quarter, where the nodes represent airports and the edges represent the routes the airline operates directed from the origin airport to the destination. A market is defined as a pair of origin and destinations, such as (OKC to LGA) regardless of the path between them. This path can be a direct flight (length of one) or involve multiple segments with connections (length greater than one). In this section we refer to an edge as a route. In the U.S. domestic market, we do not observe flights with more than three connections.

3.3.1 Edge Betweenness Centrality

The betweenness centrality (Brandes, 2008) of an edge e is the sum of the fraction of all-pairs shortest paths that pass through e:

$$C(e) = \sum_{k,l \in V} \frac{\sigma(k,l|e)}{\sigma(k,l)} \tag{3.2}$$

where V is the set of nodes, $\sigma(k,l)$ is the number of shortest (k,l)-paths, and $\sigma(k,l|e)$ is the number of those paths passing through edge e. We create a graph for each airline i at quarter t and calculate the centrality $C_i^t(e)$ for each edge. In this network, the shortest path corresponds to the path from the origin airport to the destination with the fewest connections. The centrality is interpreted as the relative number of markets (origin-destination pair) that use e as a leg.

The change in centrality is important because when connecting two airports that are endpoints of a shortest path longer than one, the centrality of all edges within that path decreases, while the centrality of the new market link increases.

Table 3.3: Network Statistics

Variable	Mean	Standard Deviation	Min	Max	Number of Observations
$\pi_{imt} > 0$	0.098	0.297	0.000	1.000	1,042,959
Centrality Change (Weighted)	-0.004	102.157	-5722.000	5430.000	1,042,959
Centrality Change (Non Weighted)	0.018	15.226	-650.622	826.629	1,042,959
Connecting Market	0.350	0.477	0.000	1.000	1,042,959

Notes: Centrality is calculated using (3.2), with weighted centrality using the number of passengers as edge weights.

Table 3.3 presents network statistics. On average, airlines operate on approximately one percent of the potential 5,342 markets between 287 airports from 2017 to 2023. 35% of these routes are used in indirect flights as a leg. The mean centrality change is centered around zero, showing the shift in travel patterns. As new routes become available and utilized in various markets, the usage of other affected markets decreases.

3.3.2 Weisfeiler-Lehman Subtree Kernel

When a carrier operates on a route, it can serve multiple purposes. It can be used for a direct flight or as a leg in connecting flights. In the context of the route network, adding a new route creates additional subtrees, representing flights that use the new route as a leg. Capturing this spillover effect is essential for accurately estimating the impact of entering a single route on the entire network.

The idea behind the shared subtrees is similar to the airport present at the market's endpoints that was introduced by Berry (1990) which has been widely used in airline literature. Berry's measure is a carrier's ratio of markets served by an airline from an airport, divided by the total number of markets served from that airport by at least one carrier and then averaged over both the origin and destination. An important shortcoming of this method is that it does not consider the structure of the route network (Ciliberto and Tamer, 2009), and more importantly, it does not take into account connecting flights.

To capture these effects, we use a specialized case of the Weisfeiler-Lehman (WL) test of graph isomorphism, as introduced by Shervashidze et al. (2011). This method compares the number of shared subtrees between two graphs and enables us to construct a measure for the spillover effect of a route on an airline's own network and the competition from other airlines.

Each iteration of the Weisfeiler-Lehman algorithm replaces the label of each node with a multiset label, which consists of the node's original label and the sorted set of labels of its neighbors. This multiset is then compressed into a new, shorter label.

Formally, let R and R' be two route networks with node labels representing airports. Σ_l represents the labels at iteration l. The mapping $c_l : \{R, R'\} \times \Sigma_l \to \mathbb{N}$ assigns labels at iteration l to their number of occurrences. The Weisfeiler-Lehman subtree kernel on two graphs is defined as the inner product of feature maps:

$$WL(R, R') = \langle \phi(R), \phi(R') \rangle, \tag{3.3}$$

where $\phi(.) = (\mathbf{c}(.)_0 | \mathbf{c}(.)_1 | \dots | \mathbf{c}(.)_l)$ is the feature map constructed from vectors of c_l for each network. We use three iterations of the algorithm since flights with more than three connections are rare.

We generate a hypothetical route network for each route, in each quarter, for every airline. We modify the network by adding or subtracting one route at a time and compare it to the previous quarter. Then, we calculate the Weisfeiler-Lehman (WL) subtree kernel between the updated network and the network from the previous quarter. Next, we normalize these values by dividing by the total number of subtrees, creating a measure between 0 and 1. This measure quantifies the impact of operating a route on the airline's route network for each quarter. Higher values indicate greater similarity in terms of the number of different subtrees, which in our case translates to the number of origins and destinations. For example, when comparing two potential routes for an airline, the one with a lower value will have more potential markets to operate, or in other words, serving that route opens up more markets (or more paths to serve the current markets).

We use our generated networks to calculate the similarity between the route network of each airline and its competitors from the previous quarter. This provides us with a measure of competition that considers not only routes but also takes into account the network's structure and captures the markets served with connections.

Table 3 displays the average ratio of affected subtrees. For instance, with AA, on average, each route operated affects 0.05% of all possible routes. Given the large number of potential routes, these cover a large number of markets. The remaining columns compare the route networks of other airlines. For example, on average, a route in the AA network is affected by 15% of the routes in AS network.

3.4 Empirical Analysis

Using the variables constructed in the previous section, we can estimate Equation (3.1), where p_{imt} represent the probability of airline i, has a positive profit on the market m at quarter t, and the log odds ratio:

$$\log\left(\frac{p_{imt}}{1-p_{imt}}\right) = \gamma \boldsymbol{X}_{mt} + \boldsymbol{w}_{mt} + \psi_i + \zeta_t + \theta_m + \alpha \Delta c_{imt} D_{imt} + HS_{imt} + \hat{H}_{-imt}, \tag{3.4}$$

Table 3.4: Weisfeiler-Lehman Subtree Kernel

Carrier	HS	AS	B6	DL	F9	G4	NK	SY	UA	WN
AA	0.995	0.150	0.141	0.222	0.154	0.143	0.112	0.083	0.227	0.171
	(0.000)	(0.008)	(0.016)	(0.006)	(0.015)	(0.009)	(0.012)	(0.018)	(0.008)	(0.008)
AS	0.988		0.143	0.167	0.155	0.099	0.135	0.092	0.163	0.171
	(0.001)		(0.018)	(0.009)	(0.012)	(0.011)	(0.016)	(0.024)	(0.009)	(0.014)
B6	0.984			0.145	0.147	0.084	0.146	0.099	0.138	0.157
	(0.005)			(0.017)	(0.025)	(0.017)	(0.019)	(0.026)	(0.019)	(0.016)
DL	0.994				0.158	0.145	0.116	0.087	0.220	0.168
	(0.000)				(0.014)	(0.007)	(0.014)	(0.020)	(0.006)	(0.008)
F9	0.987					0.102	0.137	0.092	0.157	0.177
	(0.003)					(0.014)	(0.021)	(0.022)	(0.012)	(0.013)
G4	0.992						0.074	0.052	0.146	0.105
	(0.000)						(0.009)	(0.022)	(0.006)	(0.012)
NK	0.978							0.089	0.115	0.140
	(0.004)							(0.023)	(0.013)	(0.019)
SY	0.956								0.089	0.093
	(0.018)								(0.018)	(0.021)
UA	0.994									0.171
	(0.000)									(0.008)
WN	0.989									
	(0.001)									

Notes: Standard deviations are presented in parentheses. Values are calculated based on Equation 3.3 and range between 0 and 1, where values closer to 1 indicate a higher ratio of affected subtrees in market operations. The 'HS' column compares with the airline's own route network, while the remaining columns represent pairwise comparisons with competitors.

which takes the form of a binary logit and we maximize the likelihood function:

$$\mathcal{L}(\Theta|S,R) = \prod_{i\in N}\prod_{t\in T}\prod_{m\in M} p_{imt}^{\pi_{imt}} \times (1-p_{imt})^{1-\pi_{imt}}, \tag{3.5}$$

The first step of estimation involves estimating $\hat{H}_{-imt}$. Initially, we specify that all the route importance measures of competitors, which we calculated in section 3.3.2, directly enter the likelihood function. This is similar to airline literature that controls for the competition at the market level (Ciliberto and Tamer, 2009; Ciliberto and Zhang, 2017). We then estimate the competition effect using logistic regression, controlling for the measures constructed in Section 3.3.2, as well as market fixed effects, and time fixed effects.

One challenge in estimating Equation (3.5) is the potential for incidental parameter bias because our study covers 28 quarters and more than 5000 markets. Since the panel is short and we control the market fixed effect, we apply the analytical correction method developed by Fernández-Val and Weidner (2016), which helps to mitigate this bias. All tables report the bias corrected estimates but we include a table comparing the average partial effects of our estimates with those obtained from an OLS estimation in Table A3.1. The OLS estimates, being linear, are not subject to incidental parameter bias. The bias-corrected coefficients closely align with the OLS estimates, indicating that the number of observations is large enough and our method effectively addresses the incidental parameter bias.

Columns (1) and (2) of Table 3.5 present the estimation results of (3.5), including the route importance for competitors as covariates ($\sum_{i\neq j} H_{ij}$). Columns (3) and (4) show the results using the estimated competitor importance ($\hat{H}_{-imt}$). Columns (1) and (3) use the non-weighted centrality measures, and columns (2) and (4) utilize the weighted measures.

Our results indicate that if a market is used as a leg in other markets, the likelihood of

Table 3.5: Estimation Results

	(1)	(2)	(3)	(4)
Connecting Market	4.180***	4.058***	2.401***	2.298***
	(0.016)	(0.016)	(0.025)	(0.022)
Centrality Change (Non Weighted)	0.075***		0.063***	
	(0.001)		(0.001)	
Centrality Change (Non Weighted)	−0.042***		−0.008***	
× Connecting Market	(0.001)		(0.001)	
Centrality Change (Weighted)		0.009***		0.007***
		(0.000)		(0.000)
Centrality Change (Weighted)		−0.007***		−0.005***
× Connecting Market		(0.000)		(0.000)
Spillover	39.854***	42.083***	7.883***	7.600***
	(3.028)	(2.966)	(2.623)	(2.446)
Population	3.555***	3.280***	11.628***	9.347***
	(0.342)	(0.333)	(0.535)	(0.495)
Per Capita Income	0.392*	0.230	2.337***	1.960***
	(0.220)	(0.214)	(0.350)	(0.324)
Wage	0.375***	0.484***	0.662***	0.928***
	(0.093)	(0.090)	(0.149)	(0.137)
Unemployment Rate	−0.060***	−0.053***	−0.272***	−0.257***
	(0.008)	(0.008)	(0.013)	(0.011)
No. Freezing Days	0.003**	0.002	0.002	0.001
	(0.002)	(0.002)	(0.003)	(0.002)
Snow	−0.005	−0.005	−0.007	0.000
	(0.004)	(0.004)	(0.007)	(0.006)
Precipitation	−0.002	−0.017***	−0.019**	−0.055***
	(0.005)	(0.005)	(0.007)	(0.007)
Average Temperature	−0.026	−0.135***	−0.085	−0.336***
	(0.044)	(0.041)	(0.078)	(0.064)
Maximum Temperature	0.010	0.066***	0.033	0.154***
	(0.022)	(0.021)	(0.039)	(0.032)
Minimum Temperature	0.022	0.082***	0.060	0.205***
	(0.024)	(0.022)	(0.041)	(0.034)
$\hat{H}$			10.689***	9.763***
			(0.042)	(0.037)
Carrier FE	Yes	Yes	Yes	Yes
Year Quarter FE	Yes	Yes	Yes	Yes
Market FE	Yes	Yes	Yes	Yes
$H_{i \neq j}$	Yes	Yes	No	No
Number of Observations	1,042,959	1,042,959	1,042,959	1,042,959

Notes: Statistical significance levels are denoted as follows: *** indicates significance at the 1% level, ** at the 5% level, and * at the 10% level. Standard errors are enclosed in parentheses.

serving that market increases. This effect is consistent across our specifications but when using the estimated competition measure, the magnitude of this effect is smaller.

A higher change in centrality increases the likelihood of serving a market. This increase in centrality can result from either connecting the origin or destination of a market with a direct flight or adding more routes that use the market as a connecting leg. As discussed in Section 3.3.1, betweenness centrality measures the fraction of paths passing through a market, so an increase in centrality means more routes use that market. The effect is larger when using unweighted centrality because we consider all possible routes equally. However, some connecting flights might be feasible for an airline but are not attractive to passengers and are therefore rarely used in practice.

The interaction of centrality and connecting flights captures the market that became more central in the route network that serves as connecting legs for other markets. This interaction negatively impacts the likelihood of serving those routes.

Our spillover measure is higher when a route creates more opportunities to serve markets between airports already in the network. This suggests that having more pathways to serve existing markets is more valuable than expanding to new airports. For example, this flexibility allows airlines to redirect traffic to alternative routes if an airport along the path experiences inclement weather. The effect is consistently positive and significant across all our specifications, though it is smaller when we use the predicted competition measure.

Population captures the market size and positively impacts the likelihood of serving the market. Both wages and per capita income reflect economic opportunities and also have a positive impact on the likelihood of serving the market, while the unemployment rate negatively affects it. The magnitudes of these measures are larger in columns (3) and (4).

Higher snowfall and the number of freezing days do not have a significant impact. Higher

Table 3.6: Estimation Results for Majors and LLCs

	(1)	(2)	(3)	(4)
Connecting Market	2.081***	2.080***	2.631***	2.628***
	(0.038)	(0.037)	(0.032)	(0.032)
Centrality Change (Weighted)	0.003***	0.003***	0.010***	0.010***
	(0.000)	(0.000)	(0.000)	(0.000)
Centrality Change (Weighted)	−0.002***	−0.002***	0.013***	0.013***
× Connecting Market	(0.000)	(0.000)	(0.000)	(0.000)
Spillover	155.322***	158.704***	12.774***	13.206***
	(26.839)	(25.894)	(2.496)	(2.489)
Population	17.297***	17.390***	6.793***	6.958***
	(0.880)	(0.848)	(0.627)	(0.628)
Per Capita Income	2.593***	2.591***	1.297***	1.362***
	(0.515)	(0.500)	(0.437)	(0.437)
Wage	1.536***	1.519***	0.425**	0.438**
	(0.219)	(0.212)	(0.181)	(0.181)
Unemployment Rate	−0.458***	−0.461***	−0.132***	−0.135***
	(0.020)	(0.019)	(0.014)	(0.014)
No. Freezing Days	0.001	0.001	−0.002	−0.004
	(0.004)	(0.004)	(0.003)	(0.003)
Snow (Millimeters)	−0.012	−0.012	0.000	0.000
	(0.010)	(0.009)	(0.009)	(0.009)
Precipitation	0.042***	0.043***	−0.105***	−0.105***
	(0.012)	(0.012)	(0.009)	(0.009)
Average Temperature	−0.454***	−0.458***	−0.343***	−0.338***
	(0.158)	(0.152)	(0.074)	(0.074)
Maximum Temperature	0.233***	0.234***	0.164***	0.160***
	(0.079)	(0.076)	(0.037)	(0.037)
Minimum Temperature	0.253***	0.256***	0.188***	0.186***
	(0.082)	(0.079)	(0.041)	(0.041)
$\hat{H}$	10.321***	10.331***	9.794***	9.803***
	(0.073)	(0.075)	(0.065)	(0.065)
Carrier FE	Yes	Yes	Yes	Yes
Year Quarter FE	Yes	Yes	Yes	Yes
Market FE	Yes	Yes	Yes	Yes
$H_{i \neq j}$	No	No	No	No
Number of Observations	257,672	257,672	423,315	423,315

Notes: Statistical significance levels are denoted as follows: *** indicates significance at the 1% level, ** at the 5% level, and * at the 10% level. Standard errors are enclosed in parentheses.

precipitation and average temperature decrease the likelihood of serving the market, while increases in maximum and minimum temperatures increase the likelihood. These measures are only significant when we use passenger-weighted centrality. The estimated competition measure, $\hat{H}$, increases the likelihood of serving the market.

We now separate major airlines (AA, AS, DL, and UA) and LCCs (B6, F9, G4, NK, SY, and WN) to examine any differences in their route selection decisions. We use a similar specification as in column (4) of Table 3.5.

The first column of Table 3.6 presents the results when the sample is restricted to major airlines only. In column (2), we include all low-cost carriers (LCCs) as one competitor. Major airlines are more likely to serve a market if it is used as a leg in connecting flights. The spillover effect is very large, as expected, given the larger and more connected networks of major airlines. The competition effect is positive and slightly larger. Market characteristics, such as population (market size) and economic prospects (wage, per capita income, and unemployment), all have larger coefficients.

Columns (3) of Table 3.6 presents the estimation results for LLCs, and column (4) includes all major airlines as a single competitor. LLCs are more likely to serve a market if it is used in a connecting flight. Although the spillover effect is large and positive, it is smaller compared to that of major airlines, which is expected due to the smaller route networks of LLCs. The effect of competition from the competitors' route network is positive but slightly smaller than that of the major airlines.

3.5 Conclusion

In conclusion, our study shows that airlines are more likely to serve a market if a route is used in a connecting flight. Both low-cost carriers and major airlines are more inclined to serve such markets, although major airlines are less likely to do so if the routes are on the periphery of their network.

Regarding the spillover effect of market entry, our study finds that the spillover effect positively influences airline entry decisions. The effect is greater for major airlines than for low-cost carriers. This aligns with our findings that airlines consider connecting routes when making their decisions, as these routes can open new markets or offer more flexible ways to serve existing markets. This strategy can help airlines manage traffic better, i.e. achieve higher airplane utilization, and avoid inclement weather.

The likelihood of market entry increases with greater competition, especially in the presence of spillover effects within competitors' route networks. Our results indicate that the impact of competition on entry likelihood is more significant among major airlines compared to low-cost carriers.

Appendix

Chapter 1 Appendixes

Table A1.1: The top 10 NFTs based on their USD value at the time of purchase.

Price Ranking	Details	Price Ranking	Details
1	Stay Free (Edward Snowden, 2021) $ 5,155,254 4/17/2021 	6	Nyan Cat $ 574,536 2/20/2021 
2	Dreaming at Dusk $ 1,822,020 5/15/2021 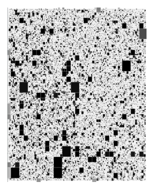	7	The New York Times x NFT $ 555,919 3/25/2021 
3	Yield by Stani x Sven Eberwein $ 1,123,294 9/10/2021 	8	x*y=k $ 531,321 3/27/2021 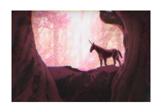
4	Coffin Dance (Dancing Pallbearers) $ 1,065,896 4/9/2022 	9	K-Meanearest Neighbors $ 506,232 10/31/2021 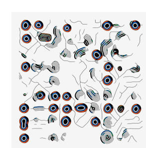
5	Finite. $ 820,818 3/14/2021 	10	Overly Attached Girlfriend $ 415,324 4/4/2021 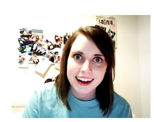

Table A1.2: Variable Descriptions

Vector	Variable	Description
y_{iast}	Log of Price	Logarithm of the winning bid value in Ethereum (ETH)
$\boldsymbol{N}_{iast}$	Centrality Seller	Measures the Katz centrality of the seller within the buyer-seller network over the past 30 days, following Equation (1.1). The network is constructed based on transactions, with the edges weighted by the value of the transactions in Ethereum.
	Centrality Buyer	Measures the Katz centrality of the buyer within the buyer-seller network over the past 30 days, following Equation (1.1). The network is constructed based on transactions, with the edges weighted by the value of the transactions in Ethereum.
	Centrality 2nd Highest Bidder	Measures the Katz centrality of the second highest bidder within the buyer-seller network over the past 30 days, following Equation (1.1). The network is constructed based on transactions, with the edges weighted by the value of the transactions in Ethereum.
$\boldsymbol{F}_{iast}$	No. of Followers Seller	The logarithm of the number of accounts following the seller on the Foundation.app platform.
	No. of Following Seller	The logarithm of the number of accounts that the seller follows on the Foundation.app platform.
	No. of Followers Buyer	The logarithm of the number of accounts following the buyer on the Foundation.app platform.
	No. of Following Buyer	The logarithm of the number of accounts that the buyer follows on the Foundation.app platform.
$\boldsymbol{S}_{iast}$	Seller Has Twitter	Indicator variable denoting whether a seller has associated their Twitter account with the Foundation platform.
	Seller Has Instagram	Indicator variable denoting whether a seller has associated their Instagram account with the Foundation platform.
	Buyer Has Twitter	Indicator variable denoting whether a buyer has associated their Twitter account with the Foundation platform.
	Buyer Has Instagram	Indicator variable denoting whether a buyer has associated their Instagram account with the Foundation platform.
$\boldsymbol{B}_{it}$	Seller is DAO	An indicator variable denoting whether the seller is a DAO.
	Buyer is DAO	An indicator variable denoting whether the buyer is a DAO.
	No. of Bidders Never Won	Count of auction participants categorized as bidders that never won an auction.
	No. of Artist and Seller	Count of auction participants categorized as both artist and seller.
	No. of Artist and Collector	Count of auction participants categorized as both artist and collector.
	No. of Collector	Count of auction participants categorized as only collectors.
	Reservation Price Change	Binary variable indicating whether the auction reservation price was changed during the auction.
$\boldsymbol{X}_{i}$	Description Length	The NFT description's length divided by 100
	Animated	An indicator variable that determines whether the NFT is animated (.MP4, .MOV, or .GIF format).
	3D	An indicator variable that determines whether the NFT is 3D (.GLB or .GLTF format).

Chapter 2 Appendixes

Table A2.1: Variable Descriptions

Vector	Variable	Description
y_{iast}	Log of Price	Logarithm of the winning bid value in Ethereum (ETH)
$\boldsymbol{N}_{iast}$	Centrality Seller	Measures the Katz centrality of the seller within the buyer-seller network over the past 30 days, following Equation (2.1). The network is constructed based on transactions, with the edges weighted by the value of the transactions in Ethereum.
	Centrality Buyer	Measures the Katz centrality of the buyer within the buyer-seller network over the past 30 days, following Equation (2.1). The network is constructed based on transactions, with the edges weighted by the value of the transactions in Ethereum.
$\boldsymbol{F}_{iast}$	No. of Followers Seller	The logarithm of the number of accounts following the seller on the Foundation.app platform.
	No. of Following Seller	The logarithm of the number of accounts that the seller follows on the Foundation.app platform.
	No. of Followers Buyer	The logarithm of the number of accounts following the buyer on the Foundation.app platform.
	No. of Following Buyer	The logarithm of the number of accounts that the buyer follows on the Foundation.app platform.
$\boldsymbol{S}_{iast}$	Seller Has Twitter	Indicator variable denoting whether a seller has associated their Twitter account with the Foundation platform.
	Seller Has Instagram	Indicator variable denoting whether a seller has associated their Instagram account with the Foundation platform.
	Buyer Has Twitter	Indicator variable denoting whether a buyer has associated their Twitter account with the Foundation platform.
	Buyer Has Instagram	Indicator variable denoting whether a buyer has associated their Instagram account with the Foundation platform.
$\boldsymbol{B}_{it}$	No. of Bidders Never Won	Count of auction participants categorized as bidders that never won an auction.
	No. of Artist and Seller	Count of auction participants categorized as both artist and seller.
	No. of Artist and Collector	Count of auction participants categorized as both artist and collector.
	No. of Collector	Count of auction participants categorized as only collectors.
	Reservation Price Change	Binary variable indicating whether the auction reservation price was changed during the auction.
$\boldsymbol{X}_{i}$	Description Length	The NFT description's length divided by 100
	Animated	An indicator variable that determines whether the NFT is animated (.MP4, .MOV, or .GIF format).
	3D	An indicator variable that determines whether the NFT is 3D (.GLB or .GLTF format).

Table A2.2: Matching Summary

	No Resale	Resale	(3)	(4)	(5)	(6)
No. of Bidder Never Won	0.096	0.163	0.136	0.147	0.169	0.138
No. of Artist and Seller	1.059	0.758	0.956	0.855	0.749	0.769
No. of Artist and Collector	1.656	2.275	2.003	2.133	2.330	2.174
No. of Collector	2.459	2.782	2.597	2.684	2.784	2.664
Price Changed	0.222	0.237	0.257	0.251	0.239	0.233
Length of NFT's Description	2.345	2.106	2.357	2.247	2.110	2.091
Animated	0.332	0.407	0.407	0.415	0.402	0.404
3D Format	0.007	0.002	0.007	0.005	0.001	0.002
Creator has Twitter	1.960	1.958	1.953	1.956	1.959	1.958
Creator has Instagram	1.749	1.774	1.772	1.787	1.771	1.782
Buyer has Twitter	1.688	1.714	1.695	1.710	1.709	1.721
Buyer has Instagram	1.310	1.371	1.368	1.373	1.378	1.368
Number of Observations	80806	1285	7710	2570	2570	2570

Notes: Each column presents the mean of the variables used in matching. Column (3)-(6) corresponds to columns in Table 2.2. In (3) and (4), distance is calculated using random forests, in (5) using logistic regression, and in (6) using Mahalanobis distance. In (3), matching selects the 5 nearest neighbors, while in the other columns, it selects the nearest neighbor.

Chapter 3 Appendixes

Table A3.1: Bias Correction Comparison

	OLS	Logit	Bias Corrected
Connecting Market	0.099***	0.303***	0.304***
	(0.001)	(0.001)	(0.001)
Centrality Change (Non Weighted)	0.004***	0.004***	0.004***
	(0.000)	(0.000)	(0.000)
Centrality Change (Non Weighted)	−0.001***	−0.002***	−0.002***
× Connecting Market	(0.000)	(0.000)	(0.000)
Spillover	2.014*	2.347***	2.350***
	(0.150)	(0.199)	(0.198)
Population	0.304***	0.210***	0.210***
	(0.014)	(0.019)	(0.019)
Per Capita Income	−0.002	0.023.	0.023.
	(0.004)	(0.013)	(0.013)
Wage	−0.010***	0.022***	0.022***
	(0.003)	(0.005)	(0.005)
Unemployment Rate	−0.005***	−0.004***	−0.004***
	(0.000)	(0.000)	(0.000)
No. Freezing Days	0.000***	0.000*	0.000*
	(0.000)	(0.000)	(0.000)
Snow	−0.001***	0.000	0.000
	(0.000)	(0.000)	(0.000)
Precipitation	−0.001***	0.000	0.000
	(0.000)	(0.000)	(0.000)
Average Temperature	−0.004*	−0.001	−0.002
	(0.002)	(0.003)	(0.003)
Maximum Temperature	0.001	0.001	0.001
	(0.001)	(0.001)	(0.001)
Minimum Temperature	0.004***	0.001	0.001
	(0.001)	(0.001)	(0.001)
Carrier FE	Yes	Yes	Yes
Quarter FE	Yes	Yes	Yes
Market FE	Yes	Yes	Yes
$H_{i \neq j}$	Yes	Yes	Yes
Number of Observations	1,042,959	1,042,959	1,042,959

Notes: The second and last columns report the average partial effects corresponding to column (1) of Table 3.5. Statistical significance levels are denoted as follows: *** indicates significance at the 1% level, ** at the 5% level, and * at the 10% level. Standard errors are enclosed in parentheses.

Table A3.2: Variables Description

π_{imt}	Link	An indicator variable denoting whether the market is served	DB1B
$\boldsymbol{X}_{mt}$	Population	The logarithm of the geometric mean of the annual population (in thousands) of the origin and destination	BEA
	Per Capita Income	The logarithm of the average annual per capita income (in thousands of dollars) of the origin and destination.	BEA
	Wage	The logarithm of the quarterly wages (in thousands of dollars) of the origin and destination.	BLS: Quarterly Census of Employment and Wages
	Unemployment Rate	The average quarterly unemployment rate of the origin and destination.	BLS: Local Area Unemployment Statistics
D_{imt}	Connecting Market	An indicator variable denoting if the origin-destination pair has been used as a segment to serve another market.	DB1B

Continued on next page

Vector	Variable	Description	Source
Δc_{imt}	Centrality Change	The difference in edge betweenness centrality from the current period to the previous period. Weighted centrality scales the centrality by the number of passengers.	Calculations are based on Equation (3.2).
HS_{imt}	Spillover	The proportion of routes impacted by operating in the market.	Calculations are based on Section 3.3.2.
$\boldsymbol{w}_{mt}$	No. Freezing Days	The number of days with maximum temperatures below 32 degrees Fahrenheit (0 degrees Celsius), calculated as the mean of the values for the origin and destination, and aggregated quarterly.	NOAA: Global Summary of the Month
	Snow	Total snowfall in millimeters, calculated as the mean of the values for the origin and destination, and aggregated quarterly.	NOAA: Global Summary of the Month
	Precipitation	Total precipitation in millimeters, calculated as the mean of the values for the origin and destination, and aggregated quarterly.	NOAA: Global Summary of the Month

Continued on next page

Vector	Variable	Description	Source
	Average Temperature	Average temperature, calculated as the mean of the values for the origin and destination, and aggregated quarterly.	NOAA: Global Summary of the Month
	Maximum Temperature	Maximum temperature, calculated as the mean of the values for the origin and destination, and aggregated quarterly.	NOAA: Global Summary of the Month
	Minimum Temperature	Minimum temperature, calculated as the mean of the values for the origin and destination, and aggregated quarterly.	NOAA: Global Summary of the Month
H_{ij}	Competition	The ratio of routes shared by airlines i and j if the market is served.	Calculations are based on Section 3.3.2.
$\hat{H}_{-imt}$	Competition	Estimated competition faced by airline i on the route.	Calculations are based on Section 3.4.

Continued on next page

Bibliography

Abadie, A. and Imbens, G. W. (2016). Matching on the estimated propensity score. *Econometrica*, 84(2):781–807.

Aguirregabiria, V. and Ho, C.-Y. (2010). A dynamic game of airline network competition: Hub-and-spoke networks and entry deterrence. *International Journal of Industrial Organization*, 28(4):377–382.

Aguirregabiria, V. and Ho, C.-Y. (2012). A dynamic oligopoly game of the us airline industry: Estimation and policy experiments. *Journal of Econometrics*, 168(1):156–173.

Alizadeh, S., Setayesh, A., Mohamadpour, A., and Bahrak, B. (2023). A network analysis of the non-fungible token (NFT) market: structural characteristics, evolution, and interactions. *Applied Network Science*, 8:38.

Ashenfelter, O. and Graddy, K. (2003). Auctions and the price of art. *Journal of Economic Literature*, 41:763–786.

Ashenfelter, O. and Graddy, K. (2006). Art auctions. *Handbook of the Economics of Art and Culture*, 1:909–945.

Athey, S. and Imbens, G. W. (2019). Machine learning methods that economists should know about. *Annual Review of Economics*, 11:685–725.

Ba, S. and Pavlou, P. A. (2002). Evidence of the effect of trust building technology in electronic markets: Price premiums and buyer behavior. *MIS quarterly*, pages 243–268.

Bajari, P. and Hortaçsu, A. (2003). The winner's curse, reserve prices, and endogenous entry: Empirical insights from ebay auctions. *RAND Journal of Economics*, pages 329–355.

Becker, G. S. (1991). A note on restaurant pricing and other examples of social influences on price. *Journal of political economy*, 99(5):1109–1116.

Beggs, A. and Graddy, K. (2009). Anchoring effects: Evidence from art auctions. *American Economic Review*, 99:1027–1039.

Benkard, C. L., Bodoh-Creed, A., and Lazarev, J. (2018). Simulating the dynamic effects of horizontal mergers: Us airlines. *Working Paper*.

Berry, S. and Jia, P. (2010). Tracing the woes: An empirical analysis of the airline industry. *American Economic Journal: Microeconomics*, 2(3):1–43.

Berry, S. T. (1990). Airport presence as product differentiation. *The American Economic Review*, 80(2):394–399.

Berry, S. T. (1992). Estimation of a model of entry in the airline industry. *Econometrica: Journal of the Econometric Society*, pages 889–917.

Bester, C. A. and Hansen, C. (2009). A penalty function approach to bias reduction in nonlinear panel models with fixed effects. *Journal of Business & Economic Statistics*, 27(2):131–148.

Bloch, F., Jackson, M. O., and Tebaldi, P. (2023). Centrality measures in networks. *Social Choice and Welfare*, 61:413–453.

Bolton, G., Loebbecke, C., and Ockenfels, A. (2008). Does competition promote trust and trustworthiness in online trading? an experimental study. *Journal of Management Information Systems*, 25(2):145–170.

Botelho, T. L. and Gertsberg, M. (2022). The disciplining effect of status: Evaluator status awards and observed gender bias in evaluations. *Management Science*, 68:5311–5329.

Brandes, U. (2008). On variants of shortest-path betweenness centrality and their generic computation. *Social networks*, 30(2):136–145.

Brueckner, J. K. (2004). Network structure and airline scheduling. *The Journal of Industrial Economics*, 52(2):291–312.

Chernozhukov, V., Fernández-Val, I., and Weidner, M. (2024). Network and panel quantile effects via distribution regression. *Journal of Econometrics*, 240(2):105009.

Ciliberto, F., Cook, E. E., and Williams, J. W. (2019). Network structure and consolidation in the us airline industry, 1990–2015. *Review of Industrial Organization*, 54:3–36.

Ciliberto, F. and Tamer, E. (2009). Market structure and multiple equilibria in airline markets. *Econometrica*, 77(6):1791–1828.

Ciliberto, F. and Williams, J. W. (2014). Does multimarket contact facilitate tacit collusion? inference on conduct parameters in the airline industry. *The RAND journal of economics*, 45(4):764–791.

Ciliberto, F. and Zhang, Z. (2017). Multiple equilibria and deterrence in airline markets. *Economic Inquiry*, 55(1):319–338.

Dai, M., Liu, Q., and Serfes, K. (2014). Is the effect of competition on price dispersion nonmonotonic? evidence from the us airline industry. *Review of Economics and Statistics*, 96(1):161–170.

De Silva, D. G., Dunne, T., and Kosmopoulou, G. (2003). An empirical analysis of entrant and incumbent bidding in road construction auctions. *The Journal of Industrial Economics*, 51(3):295–316.

De Silva, D. G., Gertsberg, M., Kosmopoulou, G., and Pownall, R. A. (2022a). Evolution of a dealer trading network and its effects on art auction prices. *European Economic Review*, 144:104083.

De Silva, D. G., Kosmopoulou, G., Pownall, R. A. J., and Press, R. (2022b). Posthumous trading patterns affecting artwork prices. *Oxford Economic Papers*, 74:453–472.

Dellarocas, C. (2005). Reputation mechanism design in online trading environments with pure moral hazard. *Information systems research*, 16(2):209–230.

Dowling, M. (2022). Is non-fungible token pricing driven by cryptocurrencies? *Finance Research Letters*, 44:102097.

Dunn, A. (2008). Do low-quality products affect high-quality entry? multiproduct firms and nonstop entry in airline markets. *International Journal of Industrial Organization*, 26(5):1074–1089.

Engelbrecht-Wiggans, R., Milgrom, P. R., and Weber, R. J. (1983). Competitive bidding and proprietary information. *Journal of Mathematical Economics*, 11:161–169.

Etter, M., Ravasi, D., and Colleoni, E. (2019). Social media and the formation of organizational reputation. *Academy of Management Review*, 44:28–52.

Fernández-Val, I. and Weidner, M. (2016). Individual and time effects in nonlinear panel models with large n, t. *Journal of Econometrics*, 192(1):291–312.

Fernández-Val, I. and Weidner, M. (2016). Individual and time effects in nonlinear panel models with large n, t. *Journal of Econometrics*, 192(1):291–312.

Fu, X., Jin, H., Liu, S., Oum, T. H., and Yan, J. (2019). Exploring network effects of point-to-point networks: An investigation of the spatial patterns of southwest airlines' network. *Transport Policy*, 76:36–45.

Gaggero, A. A. and Piazza, G. (2021). Multilayer networks and route entry into the airline industry: Evidence from the us domestic market. *Research in Transportation Economics*, 90:101044.

Gerardi, K. S. and Shapiro, A. H. (2009). Does competition reduce price dispersion? new evidence from the airline industry. *Journal of Political Economy*, 117(1):1–37.

Goolsbee, A. and Syverson, C. (2008). How do incumbents respond to the threat of entry? evidence from the major airlines. *The Quarterly journal of economics*, 123(4):1611–1633.

Grover, P., Kar, A. K., and Dwivedi, Y. (2022). The evolution of social media influence - a literature review and research agenda. *International Journal of Information Management Data Insights*, 2:100116.

Hendricks, K. and Porter, R. H. (1988). An empirical study of an auction with asymmetric information. *The American Economic Review*, 78:865–883.

Hong, H. and Shum, M. (2003). Econometric models of asymmetric ascending auctions. *Journal of Econometrics*, 112:327–358.

Hortaçsu, A. and Perrigne, I. (2021). Empirical perspectives on auctions. *Handbook of Industrial Organization*, 5.

Kane, G. C., Alavi, M., Labianca, G. J., and Borgatti, S. P. (2014). What's different about social media networks? a framework and research agenda. *MIS Quarterly*, 38:274–304.

Khademorezaian, K., Kosmopoulou, G., and Carlos, L. (2022). Networks, platforms, and auction pricing: Evidence from the nft art market. *Working paper*.

Kireyev, P. and Evans, P. C. (2021). Making sense of the NFT marketplace. *Harvard Business Review*.

Kranton, R. E. and Minehart, D. F. (2001). A theory of buyer-seller networks. *American Economic Review*, 91:485–508.

Lamarche, C. and Parker, T. (2023). Wild bootstrap inference for penalized quantile regression for longitudinal data. *Journal of Econometrics*, 235(2):1799–1826.

Lucking-Reiley, D., Bryan, D., Prasad, N., and Reeves, D. (2007). Pennies from ebay: The determinants of price in online auctions. *The journal of industrial economics*, 55(2):223–233.

Maskin, E. and Riley, J. (2000). Asymmetric auctions. *Review of Economic Studies*, 67:413–438.

Mazzeo, M. J. (2003). Competition and service quality in the us airline industry. *Review of industrial Organization*, 22:275–296.

Milgrom, P. R. and Weber, R. J. (1982). A theory of auctions and competitive bidding. *Econometrica*, 50:1089.

Nadini, M., Alessandretti, L., Giacinto, F. D., Martino, M., Aiello, L. M., and Baronchelli, A. (2021). Mapping the NFT revolution: market trends, trade networks, and visual features. *Scientific Reports*, 11:20902.

Oh, S., Rosen, S., and Zhang, A. L. (2022a). Investor experience matters: Evidence from generative art collections on the blockchain. *SSRN Electronic Journal*.

Oh, S., Rosen, S., and Zhang, A. L. (2022b). Investor experience matters: Evidence from generative art collections on the blockchain. *Available at SSRN 4042901*.

Oh, S., Rosen, S., and Zhang, A. L. (2023). Digital veblen goods. *SSRN Electronic Journal*.

Orzach, R. and Dix, R. (2021). Market power spillovers across airline routes. *Available at SSRN 3915484*.

Rapp, A., Beitelspacher, L. S., Grewal, D., and Hughes, D. E. (2013). Understanding social media effects across seller, retailer, and consumer interactions. *Journal of the Academy of Marketing Science*, 41:547–566.

Shervashidze, N., Schweitzer, P., Van Leeuwen, E. J., Mehlhorn, K., and Borgwardt, K. M. (2011). Weisfeiler-lehman graph kernels. *Journal of Machine Learning Research*, 12(9).

Vasan, K., Janosov, M., and Barabási, A.-L. (2022). Quantifying NFT-driven networks in crypto art. *Scientific Reports*, 12:2769.

Wilson, R. (1998). Sequential equilibria of asymmetric ascending auctions: The case of log-normal distributions. *Economic Theory*, 12:433–440.

Yaffe-Bellany, D. (2022). The crypto industry struggles for a way forward. *The New York Times*.

Yuan, Z. (2020). Network competition in the airline industry: A framework for empirical policy analysis. *Working Paper*.

Zhang, D. and Wang, X. (2016). Investigating the dynamic spillover effects of low-cost airlines on airport airfare through spatio-temporal regression models. *Networks and Spatial Economics*, 16:821–836.